2

Production of Optical Coatings Resistant to Damage by Petawatt Class Laser Pulses

John Bellum[1], Patrick Rambo, Jens Schwarz, Ian Smith, Mark Kimmel, Damon Kletecka[1] and Briggs Atherton
Sandia National Laboratories, Albuquerque, NM
USA

1. Introduction

There are a number of ultra-high intensity lasers in operation around the world that produce petawatt (PW) class pulses. The Z-Backlighter lasers at Sandia National Laboratories belong to the class of these lasers whose laser beams are large (tens of cm) in diameter and whose beam trains require large, meter-class, optics. This chapter provides an in-depth overview of the production of state-of-the-art high laser-induced damage threshold (LIDT) optical coatings for PW class laser pulses, with emphasis on depositing such coatings on meter-class optics.

We begin with a review of ultra-high intensity laser pulses and the various approaches to creating them, in order to establish the context and issues relating to high LIDT optical coatings for such pulses. We next describe Sandia's PW Z-Backlighter lasers as a specific example of the class of large-scale lasers that generate PW pulses. Then we go into details of the Sandia Large Optics Coating Operation, describing the features of the large optics coating chamber in its Class 100 clean room environment, the coating process controls, and the challenges in the production of high LIDT coatings on large dimension optical substrates. The coatings consist of hafnia/silica layer pairs deposited by electron beam evaporation with temperature control of the optical substrate and with ion assisted deposition (IAD) for some coatings as a means of mitigating stress mismatch between the coating and substrate. We continue with details of preparation of large optics for coating, including the polishing and washing and cleaning of the substrate surfaces, in ways that insure the highest LIDTs of coatings on those surfaces. We turn next to LIDT tests with nanosecond and sub-picosecond class laser pulses while emphasizing the need, when interpreting LIDT test results, to take into account the differences between the test laser pulses and the pulses of the actual PW laser system. We present a comprehensive summary of results of LIDT tests on Sandia coatings for PW pulses.

Two sections of the chapter present specific coating case studies, one for designs of a high reflection (HR) coating with challenging performance specifications and one for the anti-reflection (AR) coatings of a diagnostic beamsplitter. The coatings are for non-normal angle

[1] Contract Associate to Sandia (JB with Sandia Staffing Alliance; DK with LMATA Government Services)

of incidence (AOI), and the designs take into account behaviors of both S and P polarization (Spol and Ppol) electric field intensities resulting from interference of forward and backward propagating fields during reflection and transmission by the coatings. For the HR coating, a 68 layer design and a 50 layer design both meet the stringent reflectivity requirements (> 99.6% reflectivity of PW pulses in both Ppol and Spol over AOIs from 24^o to 47^o within ~ 1% bandwidth at both 527 nm and 1054 nm), but the 68 layer coating's LIDT is 5 times less than that of the 50 layer coating because the electric field exhibits high intensity peaks deep within the former coating, but exhibits peaks of moderate intensity that quench rapidly into the latter coating. The study of the AR coatings features measurements of their reflectivities, and of their uniformity over the 92 cm dimension of test optics in the coating chamber. The final section of the chapter presents a conclusion.

2. Ultra-high intensity laser pulses and approaches to creating them

Many ultra-high intensity laser facilities are in operation or under development around the world. Information on these facilities has been compiled by The International Committee on Ultra-High Intensity Lasers (ICUIL) and is available on its website, www.icuil.org. Such high intensity lasers are opening up an ever widening scope of research into laser-matter interactions beyond linear and non-linear optical phenomena at the level of molecular electronic structure and excitation to production of high energy density plasmas, energetic x-rays, inertial confinement fusion and laser induced acceleration of electrons and ions up to relativistic speeds (Perry & Mourou, 1994; Mourou & Umstadter, 2002; Tajima et al., 2010; Mourou & Tajima, 2011). Ultra-high intensity lasers depend on methods of creating laser pulses either of large energy per pulse, or of short pulse duration, or both. By large pulse energies we mean in the range from J to MJ but typically in the kJ regime for a single laser beam train; and by short pulse durations we mean in the ns, ps, fs or shorter regimes. Actually, in the world of ultra-high intensity lasers, reference to "long" in terms of pulse duration means ns class pulses; and "short" means sub-ns class pulses. The resulting intensities of these laser pulses are typically terawatt (TW) to PW and even higher. Focusing of the beams leads to corresponding fluences of 10^{16} W/cm^2 to 10^{19} W/cm^2 and beyond, approaching 10^{22} W/cm^2, depending on the particular laser system and on the achievable minimum focal spot size. Aberrations prevent focusing in the diffraction limit, so minimizing beam train aberrations is critical to achieving the highest fluences at focus. On the other hand, defocusing the beam in a controlled way is sometimes useful as a means of lowering the fluence to some specific level within a focal spot larger than the minimum achievable one.

Regardless of a laser's pulse duration/energy combination, its practical and optimal operation is feasible only to the extent that the laser pulses can traverse the beam train without causing damage or aberrations to its components (windows, mirrors, lenses, gain media, etc.) or their optical coatings. Such laser-induced damage has been the focus of extensive research (Wood, 1990, 2003). It can result from any linear or non-linear laser-matter interaction and is characterized by its LIDT, the laser fluence at or above which it occurs. Optical coatings are our particular concern, and we will deal with both HR and AR types in this chapter. HR and AR coatings are, like optical coatings in general, specific to their use wavelengths, which are the wavelengths of the ultra-high intensity lasers in this context. AR coatings consist of a few (usually < 10) alternating high and low index of refraction thin film layers while HR coatings consist of typically a few tens (< 40) of such layers. They serve the crucial role of reducing loss of energy of the laser pulses in the beam

train; in the case of AR coatings, by minimizing reflection losses at the surfaces of transmissive optics (i. e., windows or lenses) through which the pulses propagate; and, in the case of HR coatings, by minimizing transmission losses (i.e., by providing excellent reflectivities) at the surfaces of mirrors that reflect the pulses. In any case, unless these coatings as well as the optics of a laser beam train can resist damage and aberrations induced by the laser's pulses, the high energy, high intensity pulses of light will not arrive at their final focal volume efficiently enough to reach the fluence levels that produce the ultra-high energy density laser-matter interactions of interest.
The main approaches in creating ultra-high intensity laser light are as follows.

2.1 Laser systems with beam trains of large dimension and cross section

These lasers, owing to the distribution of the pulse energy over large beam cross sectional areas, can generate and handle pulses of large energies at fluences below the LIDTs of the laser optics and coatings. Such lasers, of which there about 15 around the world according to the ICUIL website, www.icuil.org, depend on major government support to provide the large facilities and infrastructure they require. They face the challenges and costs of fabricating and coating large dimension optics to high optical precision. The costs start becoming prohibitive at optic dimensions approaching a meter and beyond, especially for parabolic or other non-planar, non-spherical polished surfaces. But, because energy capacity per pulse increases linearly with beam cross sectional area, up to 4 orders of magnitude increase in pulse energies are possible in going from table top lasers with cm class beam trains to large scale lasers with meter class beam trains. Meter class laser beam trains can support kJ class energies per pulse. Perhaps the most well known of this class of lasers are the National Ignition Facility (NIF) laser system, comprised of 192 laser beam trains, at Lawrence Livermore National Laboratory (LLNL) in the United States (https://lasers.llnl.gov/), and the Laser MegaJoule (LMJ) laser system, comprised of 240 laser beam trains, at the Commissariat a l'Energie Atomique in France (http://www-lmj.cea.fr/).

2.2 Implementation of gain media, optics and coatings with superior resistance to laser-induced damage or aberrations

High LIDT gain media, optics and optical coatings are the focus of important, on-going research. Gains in energy capacity per pulse of a given laser system due to improvements in the LIDTs of optics and coatings can be significant, amounting to factors of 2 or more, but usually less than 10. As mentioned, laser-induced aberrations within gain media and optics undermine the achievement of ultra-high intensities by causing distortion of the beam's wave front and corresponding decrease of its fluence at focus. This latter effect can easily spoil the focal fluence by 1 or 2 orders of magnitude. Most ultra-high intensity lasers utilize optics and gain media with the highest fluence thresholds for laser-induced aberrations and operate at energies per pulse up to but not beyond those thresholds. They then use spatial filtering to restore the wave front of the high energy beam back closer to what it was at lower pulse energy. But, regardless of the optical medium, as laser intensities become higher and higher, the laser-induced aberrations eventually lead to local run-away self-focusing and catastrophic damage along fine, filament-like pathways (Perry & Mourou, 1994). This is due to an accumulation (referred to as the B integral) of laser-induced non-linear optical phase distortions along the propagation path, and correlates especially with intensity hot

spots that are not uncommon in the cross section of high intensity laser beams. Fused silica and BK7 are among the most laser damage resistant optical grade glasses (Wood, 2003), and Nd:Phosphate Glass and Ti:Sapphire are laser gain media that also exhibit high fluence thresholds for laser-induced damage (Wood, 2003) and at the same time afford some of the highest energy storage capacities (Perry & Mourou, 1994), at the optimal wavelengths of 1054 nm in the former case and 800 nm in the latter case. Ti:Sapphire can, however, also provide reasonable energy storage and lasing over a broad spectral range. As to thin film optical coatings, LIDTs depend not only on the coating materials but also on the coating design, on the techniques of preparing the optics for coating, and on the coating process itself. We will treat issues of coating design in more detail in this chapter. Regarding the polishing and preparing of optics for coating, we have demonstrated in the case of an AR coating that using one combination of polishing compound and wash preparation for the substrate prior to coating over another can lead to an improvement by a factor of 2 in the laser damage threshold of the coating, and hence the energy capacity per pulse of the laser (Bellum et al., 2010).

2.3 Methods of generating laser pulses of ever shorter duration

For a given energy per pulse, the intensity of the laser light varies inversely with pulse duration. So, techniques such as Q-switching or mode locking to produce short laser pulses, of ns, ps, fs, or even shorter durations, without appreciably reducing the energy per pulse, can lead to orders of magnitude increases in laser intensities.

All ultra-high intensity laser systems involve trade-offs between the above 3 approaches. Avoiding self-focusing is a major factor in any laser design. It not only limits the thicknesses of gain media and optics for given laser pulse energies and durations, but also prevents sub-ns class laser pulses produced by means of laser cavity based techniques such as Q-switching and mode locking from being able to undergo effective amplification in high energy capacity solid state gain media like Ti:Sapphire and Nd:Phosphate Glass. The reason for this latter limitation is that sub-ns pulses, as they increase in energy per pulse, reach the fluence levels resulting in self-focusing before they reach the saturation fluences necessary for efficient extraction of stored energy in the gain medium (Perry & Mourou, 1994). Due to this, the successful ultra-high intensity laser systems developed during the first few decades after the advent of the laser in the 1960s were based on approaches 2.1 and 2.2 above featuring ns class pulses. These were large laser systems using solid state gain media and generating kJ per pulse class laser beams of large, meter class dimensions, and were the predecessors of the NIF and LMJ class of lasers.

The advent of chirped pulse amplification (CPA) in the mid 1980s was a major breakthrough in opening up the realm of sub-ns ultra-high intensity laser pulses (Perry & Mourou, 1994; Strickland & Mourou, 1985; Maine et al., 1988). CPA technology uses optical gratings or other optical techniques to “stretch” a low energy sub-ps class laser pulse of sufficient bandwidth into a ps to ns class pulse, which can then undergo efficient amplification without the self-focusing problems that would occur for the sub-ps class pulse. A reverse version of the “stretching” process then recompresses the amplified ps to ns class pulse into a high energy, sub-ps class pulse. Focusing of these high energy laser pulses is the final step in achieving the ultra-high fluences of coherent light and their associated electric and magnetic optical fields that in turn lead to the high energy density laser-matter interactions. CPA with ps and fs class pulses has permitted the development of ultra-high intensity table

top lasers, but is also a technique that has become more and more common in the context of the large, meter-class, ultra-high intensity laser systems, taking them from ns pulses at TW intensity levels with 10^{18} J/cm^2 to sub-ps pulses at PW intensity levels with > 10^{21} J/cm^2.

3. The Sandia TW and PW Z-Backlighter lasers

The Z-Backlighter lasers at Sandia National Laboratories are part of the Pulsed Power Sciences program (http://www.sandia.gov/pulsedpower/) in support of the Z-Accelerator, which produces extremely high energy density conditions by means of a magnetic pinch along the vertical (Z) direction, and is the most powerful source of x-rays in the world. There are two basic Z-Backlighter lasers, Z-Beamlet (Rambo et al., 2005) with TW, ns class pulses and Z-Petawatt (Schwarz et al., 2008) with 100 TW up to PW, sub-ps class pulses. These pulses, after propagating nearly 200 feet from the Z-Backlighter Laser Facility to the Z-Accelerator, undergo focusing onto target foils near the Z pinch. Their focused fluences, ranging from 10^{16} to 10^{20} W/cm^2, produce highly energetic x-rays that back-light the magnetic pinch with enough energy to penetrate its high energy density core and, in this way, provide a diagnostic of the pinch as it occurs (Sinars et al., 2003).

The ns class Z-Beamlet laser pulses undergo multi-pass power amplification in Xe flashlamp pumped Nd:Phosphate Glass amplifier slabs at 1054 nm laser wavelength corresponding to the fundamental laser frequency of Nd:Phosphate Glass. Z-Beamlet then converts these amplified pulses by means of frequency doubling in a large dimension KDP crystal to the second harmonic at 527 nm. Its pulses are of duration in the range 0.3 – 8 ns, but the most common operation is with 1 – 2 ns pulses, and pulse energies of up to ~ 2 kJ at 527 nm in a beam of about 900 cm^2 cross sectional area. The sub-ps class Z-Petawatt laser uses optical parametric chirped pulse amplification (OPCPA). A Ti:Sapphire laser operating at 1054 nm provides 100 fs pulses at low (nJ) energies. A double-pass grating stretcher temporally expands these pulses to ~ 2 ns duration. The stretched pulses then undergo optical parametric amplification (OPA) in three stages, by means of a BBO crystal in each stage pumped by amplified, ~ 2 ns pulses at 532 nm of a frequency doubled Nd:YAG laser. After amplification in double-pass rod amplifiers, the OPA output pulses undergo final double-pass amplification in the main amplifier consisting of 10 Xe-flashlamp pumped Nd:Phosphate Glass slabs (44.8 cm X 78.8 cm X 4.0 cm). The output pulses from the main amplifier then are temporally compressed to ~ 500 fs by means of large, meter class gratings. The Z-Petawatt output pulses can range in duration down to ~ 500 fs and the energies per pulse can extend up to ~ 420 J in the current configuration that uses gratings produced on gold coated meter-class fused silica substrates. New gratings have now been produced for Sandia by Plymouth Grating Laboratory (www.plymouthgrating.com) by means of a laser based nano-ruler process (Smith et al., 2008) on large (94 cm X 42 cm X 9 cm) fused silica substrates which, prior to the nano-ruler process, were coated by Sandia with a multi-layer dielectric (MLD) coating. These new MLD gratings will permit energies per sub-ps pulse approaching 1 kJ due to their superior resistance to laser damage as compared to that of the gratings on the gold coated substrates. The expanded Z-Beamlet laser beam can present 2.5 – 10 J/cm^2 in a 1 ns pulse of 527 nm light over its cross section. In the case of the Z-Petawatt laser, the beam can present 1 - 2 J/cm^2 in a 700 fs pulse of 1054 nm light over its cross section. Our goal in large optics coatings is that their LIDTs exceed these fluences, and preferably by factors of ~ 2 in order to handle hot spots in the beams.

4. Depositing high LIDT coatings at Sandia's large optics coating operation

Coating large optics goes hand in hand with large vacuum coating chambers. In Sandia's case, the coating chamber is 2.3 m x 2.3 m x 1.8 m in size and opens to a Class 100 clean room equipped for handling and cleaning the large optics for coating (see Fig. 1). Such a highly clean environment, with downward laminar air flow into a perforated raised floor to enhance the laminar quality, is critically important to the production of optical coatings exhibiting the highest possible LIDTs. This is due to the fact that even nano-scale particulates on an optical surface prior to coating become initiation sites for laser damage of the coated surface to occur at lower LIDTs (Stolz & Genin, 2003). A major issue with particulates is that, when the coating chamber is not under vacuum and its door is open, coating material on the chamber walls tends to flake off, violating Class 100 conditions inside and in front of the chamber. This calls for measures to prevent these particulates from contaminating the surfaces of product optics prior to coating. One such measure is the use of clean room curtains, as shown in Fig. 1, to separate the area in front of the coater from the rest of the Class 100 area, shown in Fig. 2, in which optics undergo cleaning and preparation for coating. Another such measure is to handle optics in preparation for coating and to load them into the chamber using special tooling and techniques that protect the surfaces undergoing coating from exposure to the non-Class 100 conditions in front of and inside the open chamber. Once the chamber door is closed, the downward laminar flow of Class 100 air quickly restores the area in front of the chamber to Class 100 status; and the risks of particle contamination inside the chamber are negligible when it is under vacuum.

Fig. 1. The Sandia large optics coating chamber and process control console.

Among deposition methods that produce high quality coatings, conventional electron beam (e-beam) evaporation of thin film materials is the most suitable for coating large optical substrates. This is because of the high levels of uniformity of the coating over large substrate areas that are achievable with e-beam deposition due, in part, to the relatively large cone angles of the plumes of e-beam evaporated coating molecules. In addition, motion of the substrates in planetary fixtures as well as masks with special design and placement between the thin film material sources and the substrates are necessary as a means of controlling and averaging out the deposition to insure uniform thin film layer thicknesses. In Sandia's 3-planet configuration, as shown in Fig. 3, each planetary fixture can hold optical substrates up to 94 cm in diameter. The planet fixtures of a 2-planet, counter-rotating option, can hold substrates up to 1.2 m in one dimension and 80 cm in the other. The coater has three e-beam sources (see Fig. 3) for evaporation of the thin film materials. Hafnia and silica are, respectively, the high and low index of refraction layers of choice for high LIDT coatings, due to their high resistance to laser damage by visible and near infra-red light (Fournet et al., 1995; Stolz & Genin, 2003; Stolz et al., 2008). Crystal sensors in locations on the bottom sides of the masks, which are near the plane of the optical surfaces undergoing coating, serve to monitor the coating process by detecting the amount and rate at which they accumulate coating material during deposition. The Sandia chamber also can accommodate optical monitoring of the coating deposition process. An RF ion source (see Fig. 3) provides the option of IAD. The base pressure of the coating chamber needs to be ~ 1 – 2 X 10^{-6} Torr in order to insure contamination free conditions for the deposition process.

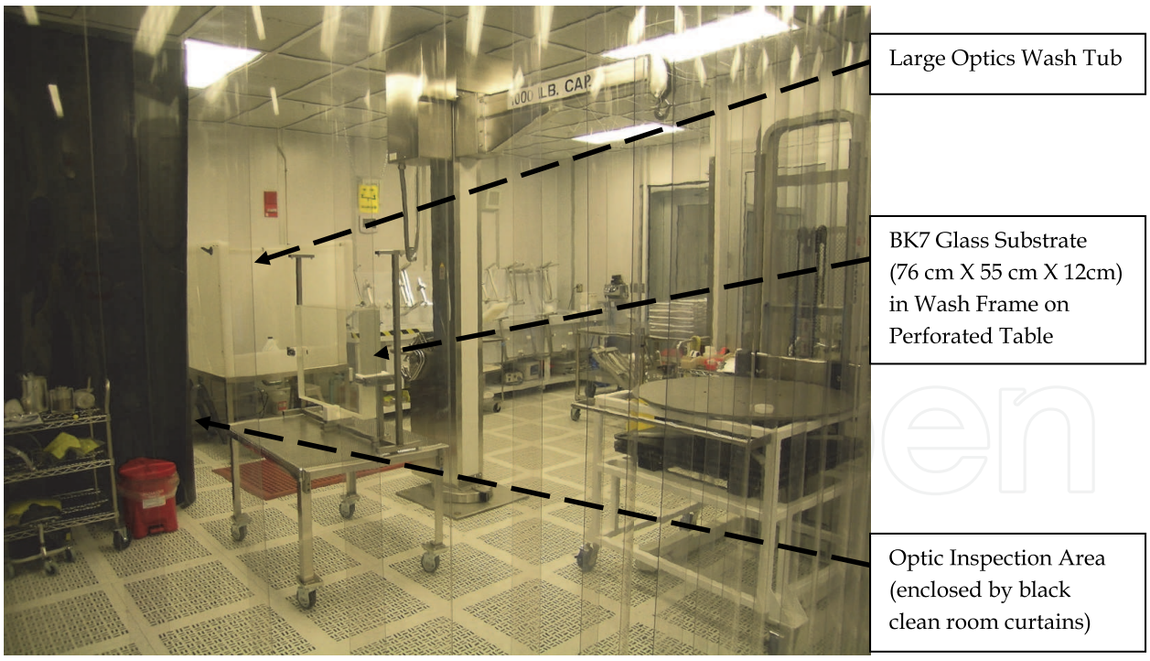

Fig. 2. Sandia's Class 100 clean room for washing and preparing large optics for coating.

Achieving high LIDT coatings depends not only on use of coating materials with high resistance to laser damage, but also on the methods of preparing the substrate surfaces for coating and on the deposition processes and process control, as we mentioned above, and, as we will see later in the chapter, on the coating design. Direct e-beam evaporation of silica,

because it occurs at moderate e-beam current and voltage, leads to generally defect-free thin film layers. This is, however, not the case for hafnia because it requires much higher e-beam current and voltage to evaporate, which in turn increases the risk of the evaporation process producing hafnia particulates along with hafnia molecules. Such particulates that attach to the coating as it is forming become defect sites that can initiate laser damage. To avoid this, we use direct e-beam evaporation of hafnium metal in combination with a back pressure of oxygen at ~ 10^{-4} Torr that is sufficient to insure that all of the evaporated hafnium atoms react with oxygen to form hafnia molecules that then form the hafnia coating layer. This occurs in a defect-free way because evaporation of hafnium metal occurs at more moderate e-beam current and voltage than evaporation of hafnia, with correspondingly lower risk of producing particulates in the evaporation process.

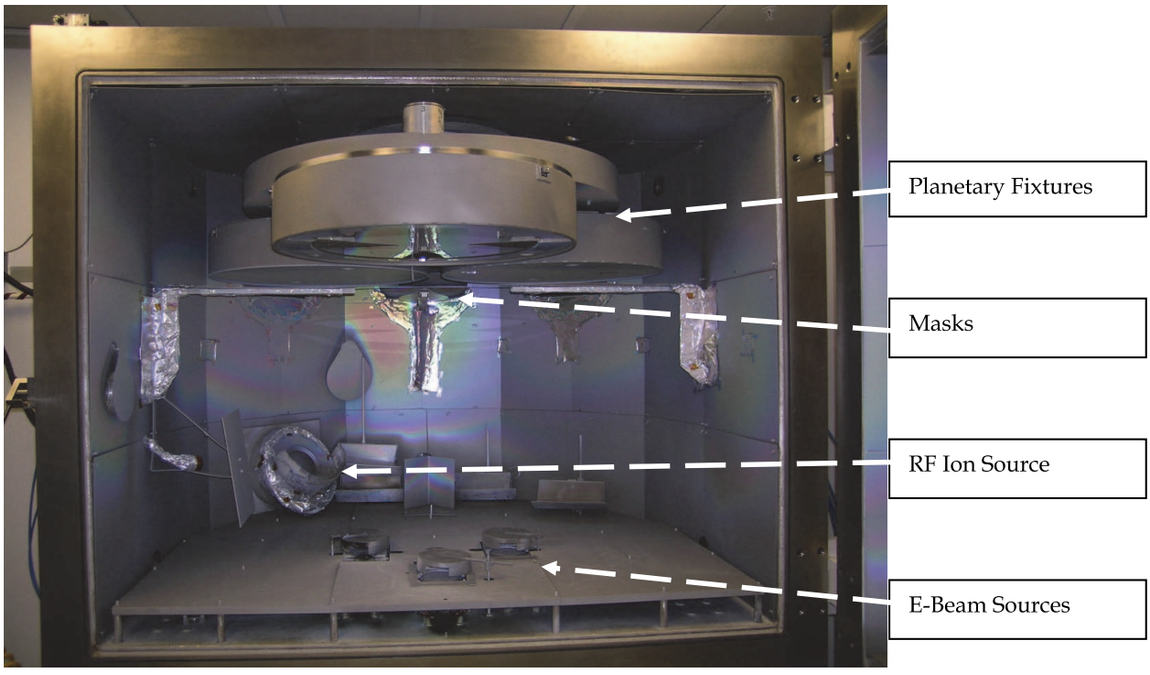

Fig. 3. Interior of the Sandia large optics coating chamber.

A feature of the Sandia large optics coater is the control of the substrate temperature - that is, the temperature within the coating chamber - during deposition. The temperature governs the energy of molecular motion, both of the coating molecules as they assemble to form a coating layer and of the substrate molecules in their phonon degrees of freedom. Thus, lowering or raising the temperature can change the dynamics at the molecular level by which coatings form. In particular, coating at an elevated temperature of ~ 200 ^{o}C can promote formation of coatings with mechanical stress (Strauss, 2003) that matches or is close to that of the substrate. This is important because stress differences between a coating and substrate increase the risk of the coating delaminating from the substrate. The case of HR coatings on BK7 optical glass is a good example of how deposition at ~ 200 ^{o}C results in low stress differences between coating and substrate. With IAD, ions from the ion source bombard the coating layer as it forms, thus modifying how the coating molecules assemble into a layer. Such IAD coatings are usually denser with a higher level of surface roughness, and have less stress mismatch with the substrate, than do non-IAD e-beam deposited coatings, and their LIDTs tend to be as high as

or somewhat higher than those of non-IAD coatings. The increase in surface roughness leads to diffuse reflection, detracting from the specular reflection that an HR coating could otherwise provide. We have investigated techniques of reducing the surface roughness of IAD HR coatings based on using an elevated chamber temperature during the coating run and on turning the ion beam off during the pause between layers in the deposition process (Bellum et al., 2009).

The risks of system or process failures in a coating run increase with the number of coating layers being deposited whether the coating system is large or small, and process control measures constitute the primary means of mitigating these risks. There are, however, additional risks and challenges when it comes to coating large optics. The amounts of thin film material that must be evaporated by the e-beam process increase with the size of the coating chamber to the extent that depletion of coating materials starts becoming a problem in a large optics coating run after ~ 20 coating layers. Related to material depletion is the problem that the topology of the depleted material's surface melt or glaze becomes irregular, and this can cause random steering of the plume of e-beam evaporated material and lead to degradation of coating uniformity. This is especially the case in the deposition of silica in that more silica must undergo evaporation to form a layer of a given optical thickness because of silica's lower index of refraction and thin film density compared to hafnia. For this reason, we use two e-beam sources for silica so that material depletion is less for each source since it needs to provide for only half the number of silica layers in a coating run. An associated challenge is achieving layer pair thickness accuracy. Though layer pair thickness errors tend to be random, the overall effect of the errors increases with number of layers. This is not so critical for standard quarter-wave layer coatings because for each layer that is a bit thinner than a quarter of a wave there is likely to be one that is a bit thicker, and the errors tend to cancel out. It is, however, critical for non-quarter-wave coatings of more than ~ 20 layers in which layer pair thickness accuracy is important especially in the outer (last deposited) layers. Figure 4 summarizes these large optics coating production challenges. Successful production of coatings on large optical substrates requires ongoing efforts to find ways of meeting and mitigating these challenges through coating process control measures.

5. Preparation of large optics for coating – polishing, washing and cleaning

Because of their size, large optical substrates usually undergo single-sided pitch polishing. For optics with optically flat side 1 and side 2 surfaces, double-sided polishing is very effective, but cannot yet handle optics of dimension more than ~ 0.6 m. Polishing large optics to scratch/dig (American National Standards Institute, 2006, 2008) surface qualities of 30/10 and surface figures of $1/10^{th}$ wave peak-to-valley is achievable, but at significant costs and lead times (often more than a year) for the fabrication and polishing processes. Going beyond these optical surface properties moves fabrication and polishing costs and lead times from significant to daunting.

The polishing compound itself influences the laser damage properties of an optically polished substrate, whether coated or uncoated, because residual amounts of it remain to some extent embedded in the microstructure of the polished surface. Alumina, ceria and zirconia are some of the most laser damage resistant polishing compounds, and this correlates in part to their sizable energy thresholds for electronic excitation and ionization. But laser damage also correlates to the degree to which trace levels of polishing compound

remain in the microstructure of a polished surface, which in turn depends on the hardness and size of the polishing compound particles. In any case, the achievement of the highest possible laser damage threshold for a coated optic depends on techniques of washing and cleaning the optical surface prior to coating in a way that removes as much surface contamination as possible, including residual polishing compound.

At Sandia, washing of meter-class optics is by hand in the large optics wash tub (see Fig. 2) following the wash protocol of Table 1. Inspection of the cleaned surfaces is by eye in the dark inspection area (see Fig. 2) using bright light emerging from a fiber optic bundle within a small cone angle to illuminate the optic surfaces. For large optics, such manual washing and inspection are most common, although hands-off, automated wash and inspection processes offer advantages and are becoming available (Menapace, 2010). The first 8 steps of Table 1 include an alumina slurry wash step along with mild detergent wash and clear water rinse steps. This protocol relies on copious flow of highly de-ionized (DI) water (resistivity > 17.5 MΩ) and on washing using ultra-low particulate hydro-entangled polyester/cellulose Texwipes. The mild detergent is Micro-90 diluted with DI water. The alumina slurry is Baikalox (also under the name, Rhodax) ultra pure, agglomerate free, 0.05

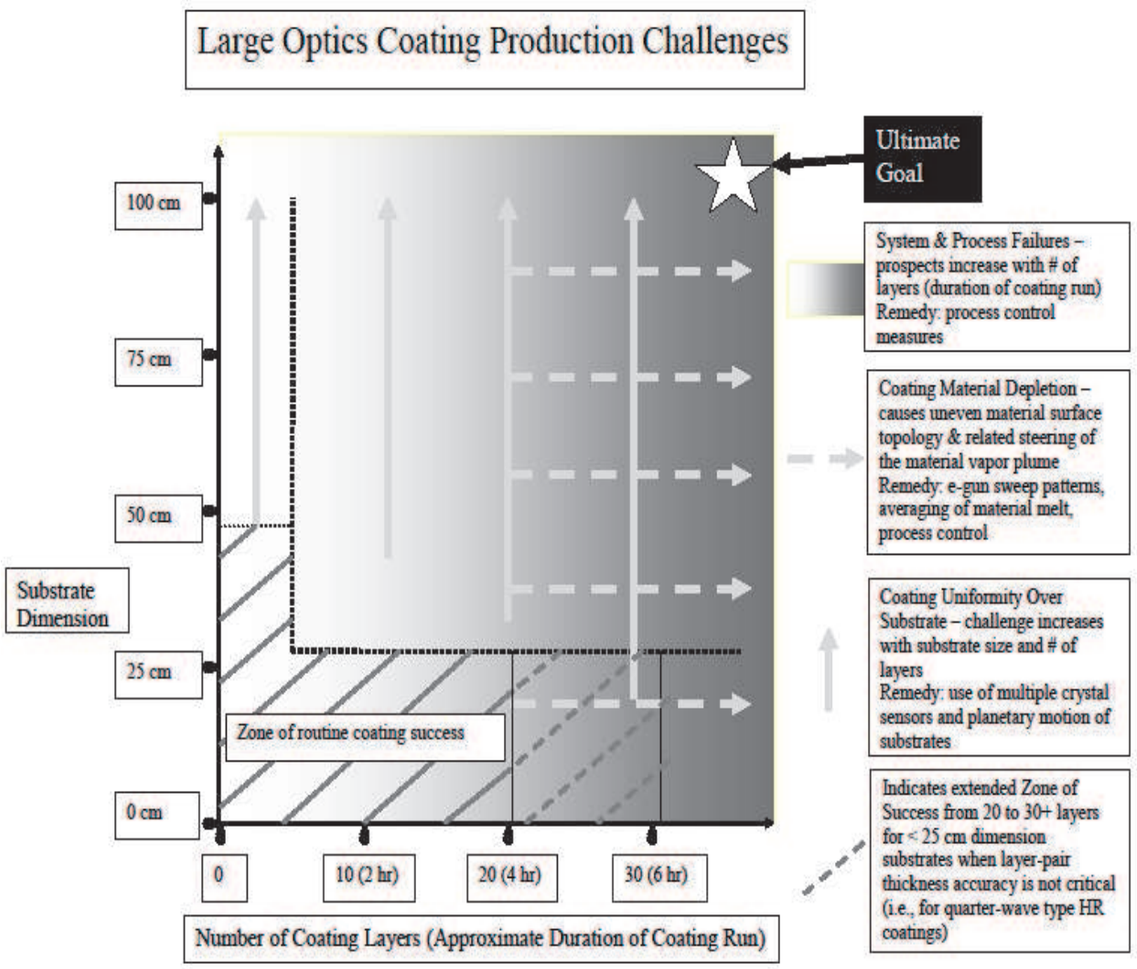

Fig. 4. Summary of large optics coating production challenges.

CR alumina polishing liquid, which is a suspension of alumina particles with nominal size of 0.05 μm. Washing using the slurry with its extremely fine alumina particles serves to remove, at least partially, the residual polishing compound embedded in the microstructure of the optical surface, and does so without degrading the optically polished surface's scratch and dig properties. This is important because polishing compounds are usually less resistant to laser damage than are the optical surfaces or the coatings, so removing residual polishing compound can enhance the LIDT of the coated surface. Our recent study on this (Bellum et al., 2010) found that LIDTs of an AR coating on fused silica substrates polished with ceria or zirconia polishing compounds were ~ 2 times higher for the substrates we washed with compared to without the alumina wash step, confirming that the alumina slurry wash step significantly reduces residual polishing compound on the optic surface and leads to improved LIDTs of coatings on those surfaces.

The steps of Table 1 proceed with repetition as necessary until Step 9, the Class 100 laminar air flow drying, occurs with the optic surface properly sheeting off excess DI water and being free of any cleaning residue or particles as verified by Step 10. In Step 11, the optic either passes inspection or fails, in which case we return to Step 1. An optic that passes inspection should, within hours the same day, be loaded into the chamber for coating. Otherwise it must undergo the wash process again because the risks of particulates attaching to its surface become unacceptably high even after a few hours in the Class 100 environment. In Step 9, the washed substrate rests in its wash frame, as shown for the BK7 substrate in Fig. 2, such that the laminar air flow occurs along the washed surfaces. Use of a perforated table, like that of Fig. 2, on which to place the washed optics helps maintain the laminar quality of this downward air flow at the high level required to prevent particulates from attaching to the optical surface to be coated. As we mentioned earlier, keeping the surface free of particulates is necessary to achieving the highest laser damage resistance of the eventual coating on the surface, since such particulates serve as likely sites for initiation of laser damage.

Step 1.	Clear water rinse/wipe
Step 2.	Vigorous mild detergent wash
Step 3.	Clear water flow rinse
Step 4.	Vigorous alumina slurry wash
Step 5.	Clear water flow rinse
Step 6.	Vigorous mild detergent wash
Step 7.	Vigorous clear water wash/rinse
Step 8.	Thorough clear water flow and/or spray rinse
Step 9.	Class 100 laminar air flow drying
Step 10.	Inspection of washed optic
Step 11.	Optic passes – or return to Step 1

Table 1. Large Optics Wash Protocol

6. LIDT tests

Laser-induced damage to optics and their optical coatings varies greatly as to the mechanisms by which it occurs (Wood, 1009, 2003), as to whether it does or does not grow or propagate in physical size, and as to how deleterious its effects are to the operation of a laser. These

variations depend on factors such as the frequency (i.e., wavelength) of the laser light, its transverse and longitudinal mode structure, the duration and temporal behavior of the laser pulse, and the laser fluence. The LIDT refers to the maximum laser fluence, usually expressed in J/cm^2, that a coated optic in a given laser beam train can tolerate before it suffers damage to an extent that prevents satisfactory operation of the laser. LIDT tests should ideally take place with the actual optic in the actual laser of interest which, in the present context, is a PW class laser with meter-class optics. This is, however, not practical. Instead, LIDT tests are commonly done on small damage test optics using table top high energy lasers whose laser wavelength, transverse and longitudinal mode structure, and pulse duration and temporal behavior are similar to those of the ultra high intensity laser of interest. Such damage test lasers need only be capable of producing moderately high intensity laser pulses whose fluences can, with focusing if necessary, range up to and beyond those expected in the transverse beam cross section of the ultra high intensity laser. For the LIDT tests to be as valid and informative as possible, the damage test optic must match the large, meter-class laser optic in type of optical glass, in polishing compound and process, in washing and cleaning prior to coating, and in optical coating, including that both the test optic and the meter-class optic be coated in the same coating run. Even so, because of differences between the test and use lasers, results of LIDT tests require careful interpretation in determining how they relate and apply to the design and performance of a given PW class laser.

By convention, LIDTs are the fluences as measured in the laser beam cross section regardless of whether or not the AOI of the laser is normal to the coated optical surface. Thus, the measured LIDT fluence projects in its entirety onto the optic surface only for LIDT tests at normal AOI. For LIDT tests with the laser beam at a non-normal AOI, the measured LIDT fluence projects only partially onto the optic surface, with the corresponding projected fluence on the surface being less than the measured LIDT by the geometric projection factor of cosine of the AOI. Even though this can be confusing, it is important to keep in mind. For LIDT tests to be valid for optical coatings whose designs are for specific non-normal AOIs and Spol or Ppol, the AOIs and polarization of the test laser beams must match those of the coating designs. This is especially important because of the differences in boundary conditions satisfied by Spol and Ppol components of the optical electric fields at interfaces between optical media (Born & Wolf, 1980). For coatings, these interfaces are those between the coating and the substrate, the coating and the incident medium, and the coating layers. These boundary condition differences at non-normal AOIs can lead to significant differences between Spol and Ppol LIDTs, as we have shown for various 4-layer AR coatings (Bellum et al., 2011).

The Z-Backlighter lasers operate with two pulse types: single longitudinal mode, ns class pulses at 1054 nm and 527 nm in the case of the Z-Beamlet TW class laser; and mode-locked, sub-ps class pulses at 1054 nm in the case of the 100 TW and PW class lasers. The lasers fire on a single shot basis, usually with hours between shots. Their laser beams all exhibit single transverse mode intensities resulting from spatial filtering, and also exhibit intensity hot spots across the beam cross section. LIDT tests on coatings of the Z-Backlighter laser optics are also with single transverse mode laser pulses, but with differing longitudinal mode properties. The tests at or near the 1054 nm wavelength are with multi longitudinal mode, ns class pulses or with mode-locked, sub-ps class pulses; and the tests at or near the 527 nm wavelength are with multi or single longitudinal mode, ns class pulses. Multi longitudinal mode pulses exhibit intensity spikes due to random mode beating and may for this reason

be more effective in causing laser damage at a given fluence than single longitudinal mode or mode-locked pulses, which tend to exhibit temporally smooth intensity behavior [see, for example, (Do & Smith, 2009)]. The enhancement of laser damage associated with intensity spiking in LIDT tests with multi longitudinal mode pulses tends, however, to make these tests realistic in that it is a counterpart to (though different from) actual enhancement of laser damage that occurs in the Z-Backlighter laser beam trains due to beam hot spots.

LIDT tests of Z-Backlighter laser coatings are of several types. First is an important type of long pulse test which is performed by Spica Technologies Inc. (www.spicatech.com) using 3.5 ns, multi longitudinal mode Nd:YAG laser pulses at 1064 nm or frequency doubled at 532 nm. These wavelengths are close enough to the 1054 nm or 527 nm Z-Backlighter wavelengths that LIDTs measured at 1064 nm or 532 nm reliably match those at 1054 nm or 527 nm. The pulses are incident one shot at a time per site of a 1 cm X 1 cm grid of ~ 2500 such sites on the coating. This testing protocol originated out of the NIF laser program (National Ignition Facility, 2005) and we refer to it as the NIF–MEL protocol. In the raster scans, the laser spot overlaps itself from one grid site to the next at its 90% peak intensity radius. In our tests, the fluence in the cross section of the laser beam usually starts at 1 J/cm^2 for the first raster scan and increases in increments of 3 J/cm^2 for each successive scan. This procedure amounts to performing a so-called N:1 LIDT test (Stolz & Genin, 2003) at each of the ~ 2500 raster scan sites over the 1 cm^2 area, conducted by means of raster scan iterations with the fluence increasing iteration to iteration. At each fluence level, the test monitors the number of new laser induced damage sites, of which there are two basic types; those that are non-propagating in that they form but then do not grow in size as the laser fluence increases, and those that are propagating in that they form and then continue growing in size as the laser fluence increases. The NIF-MEL protocol specifies the LIDT as the lowest between the two fluence thresholds, the propagating damage threshold for which at least one propagating damage site occurs, or the non-propagating damage threshold for which the number of non-propagating damage sites accumulates to at least 25, corresponding to non-propagating damage over ~ 1% of the 1 cm^2 scan area (~ 1% of the ~ 2500 scan sites). This LIDT protocol indicates the damage behavior we can realistically expect of a coating when it is in the laser beam train exposed daily to Z-Backlighter laser shots. The propagating damage threshold specifies the fluences at which we can avoid catastrophic coating failure resulting from one or more propagating damage sites. Such propagating damage typically grows into large damage craters and definitely constitutes an unacceptable degradation to the coating's optical performance. The non-propagating damage threshold, on the other hand, specifies the fluences at which we can keep the area coverage of non-propagating damage to the coating at ~ 1% or less of the area of the coating exposed to the laser beam. This 1% gauge is based on an estimate of when non-propagating damage becomes unacceptable. As the area coverage of non-propagating damage increases to the 1% level, we expect based solely on geometry that the optical losses due to scattering of light by the non-propagating damage sites become appreciable compared to 1% of the laser beam intensity. This approaches a level of loss that we try hard to avoid. For example, by means of AR coatings on transmissive optics we try to keep surface reflection losses below 0.5%. So, the non-propagating damage threshold is indeed a reasonable gauge for assessing the laser fluence beyond which the degradation of a coating's optical performance due to non-propagating damage is no longer acceptable.

Next are our in-house LIDT tests, which are in the short pulse regime with 350 fs, mode locked pulses at 1054 nm on a single shot basis, and in the long pulse regime with 7 ns, single or multi longitudinal mode pulses at 532 nm on a single shot basis, and also on a multi shot basis (10 shots at 10 Hz pulse repetition frequency) but only in the case of multi

longitudinal mode pulses. Our recent papers provide a detailed description of the test set-up and formats for the 350 fs pulses at 1054 nm (Kimmel et al., 2009) and the 7 ns pulses at 532 nm (Kimmel et al., 2010). For the latter in-house tests at 532 nm, the single longitudinal mode condition is achieved by injection seeding of the laser with the output of a single longitudinal mode seed laser. Within the overall long pulse regime, the pulse duration

		NIF-MEL Tests		**Sandia In-House Tests**	
	AOI	1064 nm (3.5 ns pulses)	532 nm (3.5 ns pulses)	1054 nm (350 fs pulses)	532 nm (7 ns pulses)
AR coatings					
for 1054 nm	0 deg	18, 18, 19, 19, 21, 25, 25, 27, (33)		(1.8)	
for 1054 nm	32 deg	Spol: (37); Ppol: (34)			
for 1054 nm	45 deg	Spol: 47; Ppol: 19			
for 527 & 1054 nm	0 deg	(25), ((19)), [23], [[29]], 19, 22	(9), ((6)), [8], [[13]]	[[~ 2]]	[[38]], [[38]]; 10 shot: [[28]]
for 527 & 1054 nm	22.5 deg	Spol: (38), ((46)); Ppol: (38), ((55))	Spol: (12), ((11)); Ppol: (12), ((13))		
HR coatings (quarter-wave type)					
for 1054 nm	0 deg	IAD: 37, 56, 75; Non-IAD: 82			
for 1054 nm	32 deg	Spol: (79), ((82)); Ppol: (88), ((79)), 70, 91			
for 1054 nm	45 deg	Spol: (82), ((88)), [88]; Ppol: (73), ((75)), [88], 58, 79, 88, 88, 91, 91, 97			
for 527 & 1054 nm	30 deg			Ppol: (1.32), (1.71)	Ppol: 70

Table 2. Measured LIDTs (in J/cm^2) of Sandia AR and HR coatings. For each listed coating, values in similar brackets are for the same coating run.

differences (7 ns pulses of our in-house 532 nm tests, 3.5 ns pulses of the NIF-MEL tests, and ~ 1 ns pulses of the Z-Backlighter lasers) lead to corresponding differences in LIDTs, with the longer pulses affording higher LIDTs at a given fluence than those with the shorter pulses. Finally, concerning LIDTs, the NIF-MEL criteria [see above and (Bellum et al., 2009, 2010; National Ignition Facility, 2005)] involves each raster scan site on the coating receiving multi longitudinal mode laser shots one at a time, with minutes between shots, over and over at increasing fluence until damage (non-propagating or propagating) occurs. For our in-house tests, by contrast, each new site on the coating receives either a single laser shot or 10 laser shots (at 10 Hz) at a given fluence with the next new site similarly receiving one shot or 10 shots at a higher fluence, etc., until damage occurs (Kimmel et al., 2009, 2010). In addition, the NIF-MEL laser damage test protocol, with its 2500 raster scan sites in a 1cm X 1cm area, samples an appreciable area of the coating. On the other hand, our in-house testing is at tens of specific sites on the coating with one level of laser fluence at each site, and so affords a more limited sampling of the coating. The important point is that interpretation of the various LIDT tests requires taking into account their differing conditions and relating these conditions to those of the PW laser. Table 2 summarizes results from our previous reports of these LIDT tests on Sandia coatings (Bellum et al., 2009, 2010, 2011; Kimmel et al., 2009, 2010). The LIDTs are all reasonably high and adequate to insure that the coatings will stand up to the laser fluence levels of the PW class pulses in the Z-Backlighter beam trains.

7. HR coating case study: Electric field intensity behaviors favorable to high LIDTs

A key optic in the next generation Z-backlighter laser beam train is the PW Final Optics Assembly (FOA) steering mirror. It has very challenging coating performance specifications, well beyond what we normally face, and provides an instructive coating design case study. We included an initial report on this mirror and its coating in a recent paper (Bellum, 2009). The mirror's fused silica substrate, shown in Fig. 5, is 75 cm in diameter with a sculpted back surface and corresponding thickness ranging from ~ 3 cm at the edge to a maximum of ~ 15 cm in an annular zone centered about the optic axis. It weighs ~ 100 kg, and serves as the final optic steering the Z-Backlighter laser beams to focus. Its use environment is in vacuum so its coating needs to be IAD, as we explained in the recent paper (Bellum, 2009). The Z-Backlighter reflectivity performance requirements of its HR coating are very demanding: R for Ppol and Spol > 99.6 % for AOIs from 24^o to 47^o and for both the Nd:Phosphate Glass fundamental and second harmonic wavelengths with extended bandwidths; that is for 1054 nm +/- 6 nm and for 527 nm +/- 3 nm. Furthermore, the coating's LIDT must allow it to handle the ns as well as sub-ps pulses of the Z-Backlighter lasers; namely, LIDT > 2 J/cm^2 for the sub-ps Z-Petawatt laser pulses at 1054 nm, and LIDT > 10 J/cm^2 for the ns Z-Beamlet laser pulses at 527 nm.

We begin this case study by reviewing the considerations that influence the process of designing an optical coating consisting of alternating layers of high and low index of refraction materials. Perhaps the most basic one is that of determining the layer thicknesses of the coating such that it reflects or transmits light according to design specifications for the wavelengths, AOIs and polarization of the incident light. This in turn depends on how the incident light divides up into forward and backward propagating components due to partial transmission and/or reflection at each boundary between coating layers, and on how these

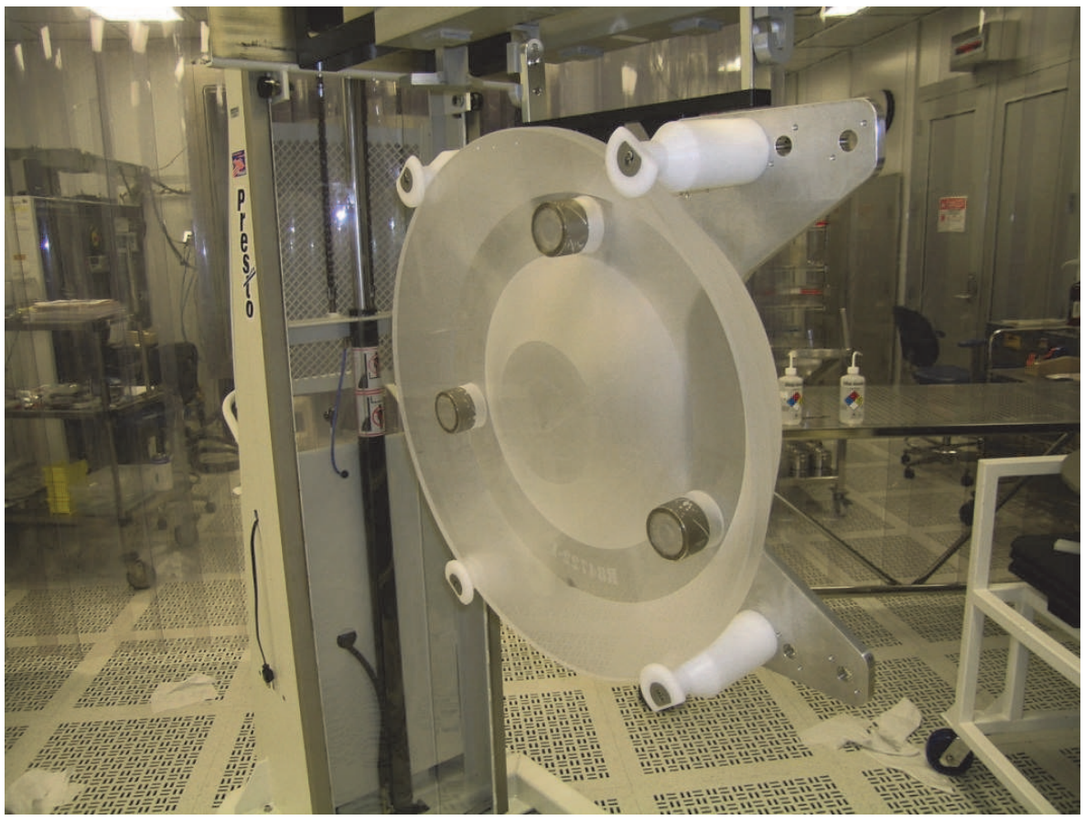

Fig. 5. The PW FOA steering mirror substrate, held by the large optics loading tool.

forward and backward propagating components interfere with one another. The perplexity of this design step is that different combinations of layer thicknesses (i.e., of interfering forward and backward propagating components of light) can lead to similar overall transmission or reflection. In other words, there is not a unique optical coating design for a given set of transmission and reflection performance criteria. Excellent coating design software codes are available. They rely on various design algorithms based on minimizing differences between design criteria and the calculated performance of the coating. The minimization procedures depend on the starting choice of layers and their thicknesses and lead to local minima. A better minimum may be achievable with a better, or just different, choice of starting layers or with a different choice of design algorithm. In the end, these software codes serve as useful tools for exploring coating design options, and the best coatings result from judicious assessment and exploration of theoretical designs by the designer based on his or her knowledge and experience with coating deposition and performance. Our design process relies on the OptiLayer thin film software (www.optilayer.com), which has proven to be a very effective tool for exploring coating design options. Other coating design considerations include how feasible it is to produce the coating on the intended product optic with the available coating deposition system and, for coatings for ultra-high intensity lasers, whether the design provides the required transmission or reflection properties with the highest possible LIDT.

Coating designs that meet the PW FOA steering mirror's daunting, dual-wavelength, and wide ranging AOI HR performance requirements will differ from standard quarter-wave

type coatings, like those we reported before (Bellum et al., 2009), that are suitable for HR at a single wavelength and AOI. Our first design attempt for the PW FOA steering mirror coating was based only on meeting the challenging HR performance goals, and resulted in a 68 layer coating about 9 μm thick. Figure 6 shows the calculated Ppol reflection spectra of this coating in spectral regions near the dual design wavelengths of 1054 nm and 527 nm for a sample of 5 AOIs, 25°, 30°, 35°, 40°, and 45°, within the coating's 24° to 47° performance range of AOIs. These calculated reflectivities confirm that the coating should very successfully meet these stringent HR performance specifications.

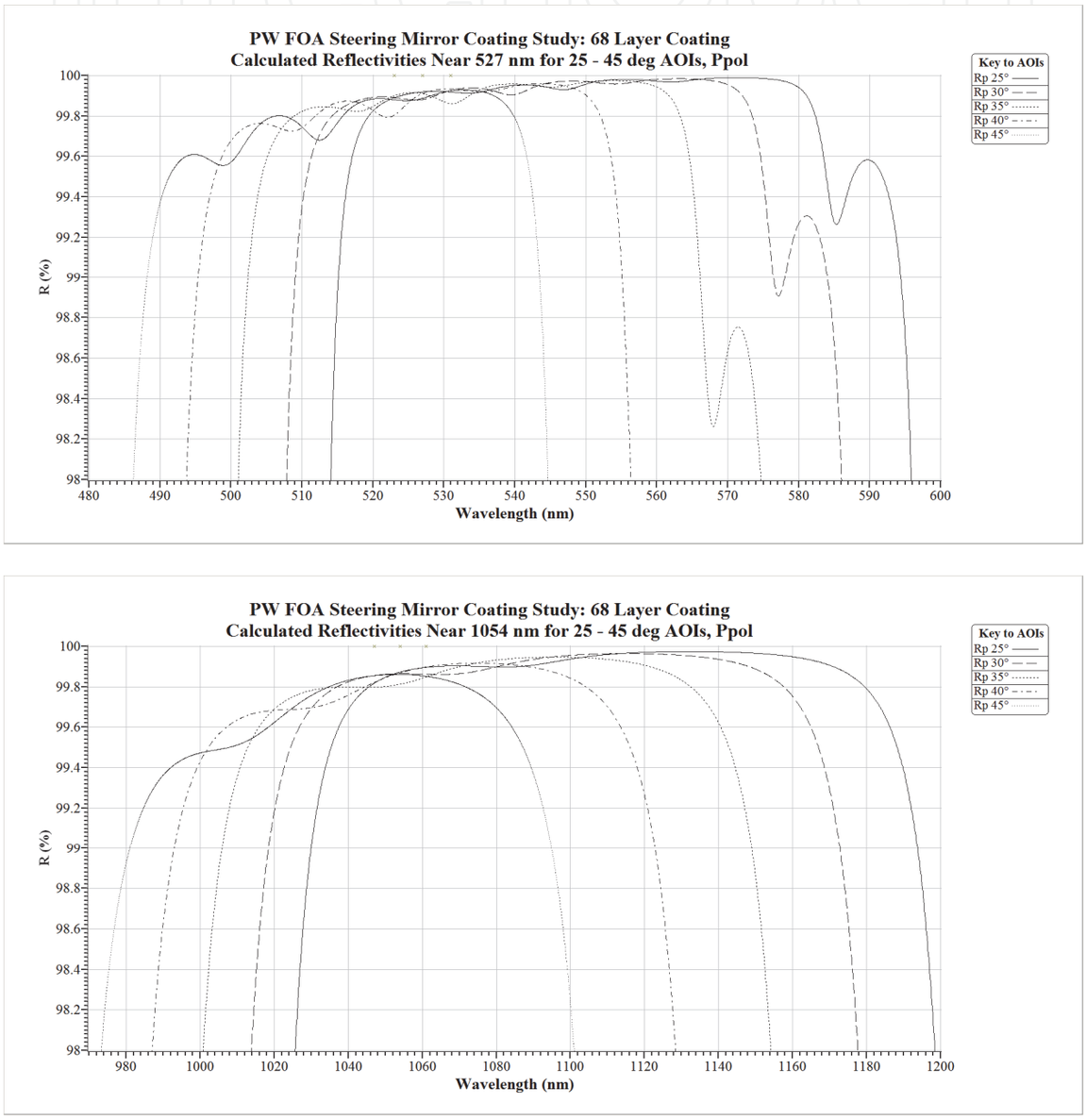

Fig. 6. Calculated reflectivities for Ppol at 25°, 30°, 35°, 40° and 45° AOIs and wavelengths near 527 nm (top figure) and 1054 nm (bottom figure) according to the 68 layer coating design for the PW FOA steering mirror.

The reflectivities of Fig. 6 indicated this 68 layer design would be a good one to use despite the risks we explained above of unforeseen coating process problems that tend to increase with the number of coating layers and process time, which is about 8 hours for this coating. But, LIDTs measured in the NIF-MEL protocol at 25°, 30° and 35° AOIs, Ppol, for this coating are all similar and proved to be disappointing at 532 nm, though excellent at 1064 nm. Figure 7 shows these LIDT results for the case of 35° AOI. The figure displays the cumulative number of non-propagating damage sites versus laser fluence and indicates by a horizontal dashed line the fail threshold of 25 non-propagating damage sites. At 1064 nm, the number of non-propagating damage sites accumulates to only 5 (with no propagating damage sites) as the laser fluence increases to 79 J/cm² (which was the highest fluence the test laser could produce in this particular test configuration). We conclude that the LIDT at 1064 nm in this case is > 79 J/cm²; which is to say that since, at 79 J/cm², neither has the number of non-propagating damage sites exceeded 25 nor has propagating damage occurred, the former will exceed 25, or the latter will occur, only at a fluence > 79 J/cm². This is a very adequate LIDT for ns class Z-Backlighter laser pulses at 1054 nm. At 532 nm, on the other hand, the non-propagating damage sites accumulate to 93, well in excess of 25, at a laser fluence of only 2.5 J/cm². This, then, is the NIF-MEL LIDT in this case, and it is well below the > 10 J/cm² required for the ns class Z-Backlighter laser pulses at 527 nm. The corresponding LIDT results at 25° and 30° AOIs are, respectively, 2.5 J/cm² and 4 J/cm² at 532 nm and, respectively, 76 J/cm² and 79 J/cm² at 1064 nm, completely consistent with their 35° AOI counterparts.

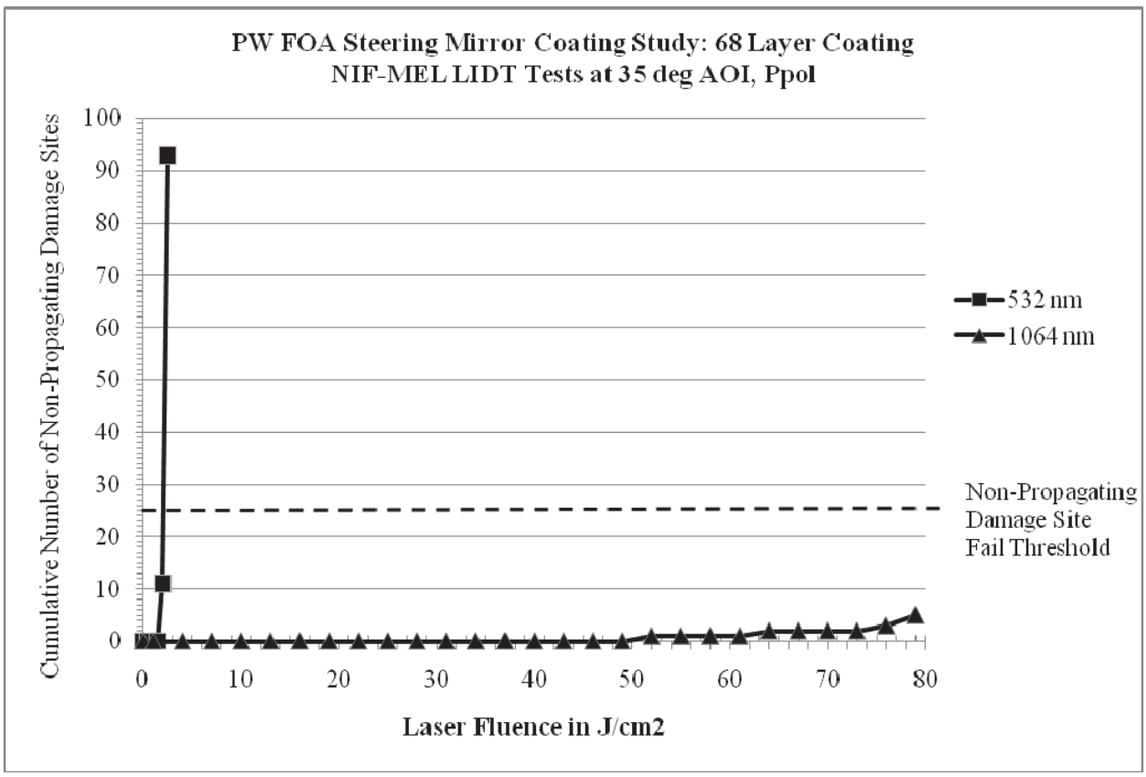

Fig. 7. NIF-MEL LIDT test results at 532 nm and 1064 nm, and 35° AOI, Ppol, for the 68 layer PW FOA steering mirror coating.

We discovered the reason for these disappointing LIDTs at 532 nm by looking at the behavior of the optical electric field intensities for this 68 layer coating. Figure 8 shows the 527 nm field intensities for the 35° AOI, Ppol case. These intensities exhibit significant ringing, with many intensity peaks over 200% of the incident intensity within ~ 34 layers into the coating, and with the highest peak at 340% of the incident intensity. The 527 nm, Ppol intensities for 25°, 30°, 40° and 45° AOIs are all similar to those of Fig. 8. This explains why this 68 layer coating suffered laser damage so readily. Its design is a set of coating layers that provide excellent reflectivities for 527 nm over the 24° to 47° range of AOIs (Fig. 6), but in a way in which highly constructive interference of the forward and backward propagating components of light occurs within the first 34 layers of the coating. This interference becomes destructive, with rapid quenching of the intensity, only within layers 34 to 46 (see Fig. 8), which is where the reflection of the 527 nm light actually takes place within the coating. This means that the 527 nm light must propagate more than half way into the coating before it reaches the layers that reflect it. And in this process, the reflected light interferes constructively with the incoming light within the first 34 layers, leading to the strong intensity peaks that in turn make the coating more susceptible to laser damage at the lower fluences.

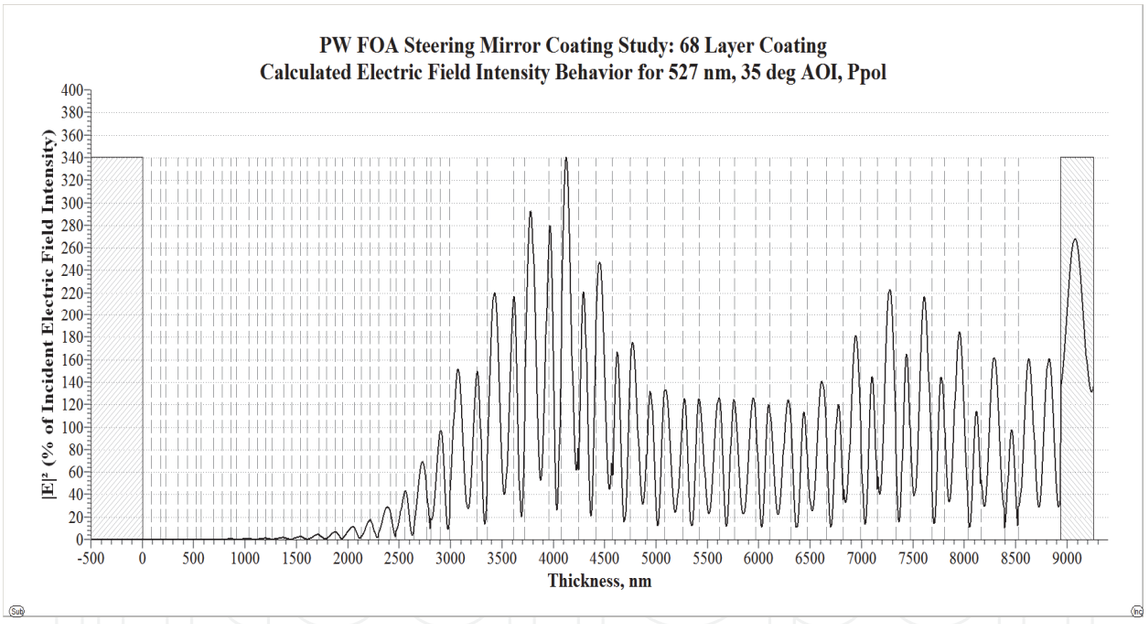

Fig. 8. Calculated electric field intensity at 527 nm for the 68 layer PW FOA steering mirror coating for 35° AOI, Ppol. Shaded areas denote the substrate (left), which is fused silica, and incident medium (right), which is air or vacuum. Vertical dashed lines mark the boundaries of the coating layers.

A very different behavior of electric field intensity is exhibited by 1054 nm light incident on this 68 layer coating, as Fig. 9 shows for 35° AOI, Ppol. The optical electric field intensity peaks quench rapidly into the coating, progressing from ~ 160% of the incident intensity in the outermost silica layer to ~ 100% by the 3nd layer and on down to < 10% beyond the 12th layer. Thus, reflection at 1054 nm is based primarily on interference between forward and backward propagating components of light within the first 12 to 15 layers of the coating,

and this interference leads to intensity peaks well below the incident intensity except in the outer silica layer where the peak is moderate, at ~ 160 % of the incident intensity. This type of electric field behavior is favorable to high LIDTs (Stolz & Genin, 2003; Bellum et al., 2009), as is confirmed by the high 1054 nm LIDTs of this 68 layer coating. The thicker outermost silica layer of this 68 layer coating is a feature of its design that enhances this type of electric field pattern for 1054 nm light favorable to high LIDTs (Stolz & Genin, 2003; Bellum et al., 2009).

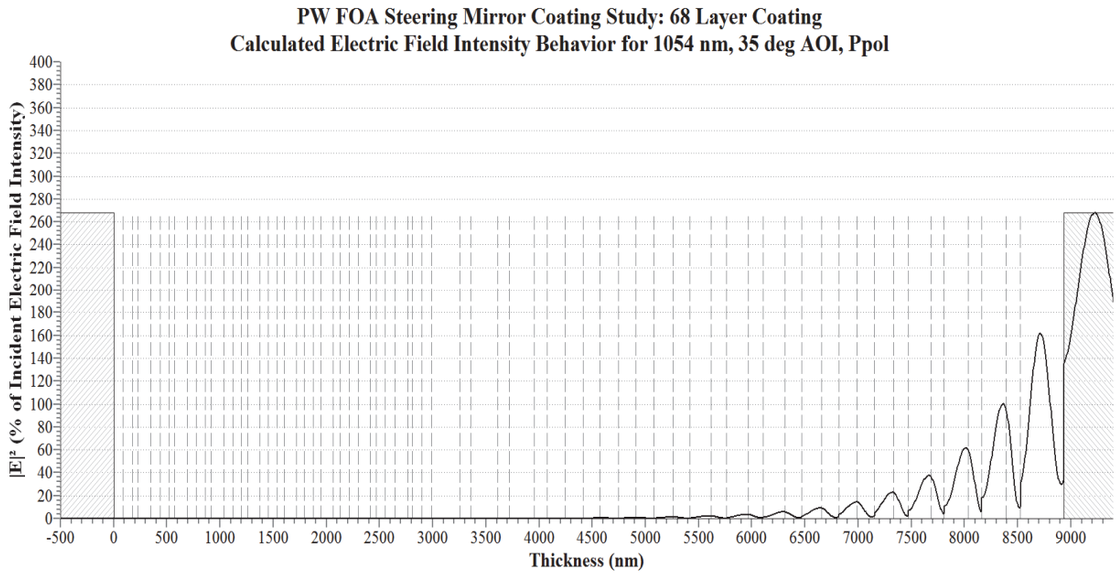

Fig. 9. Calculated electric field intensity at 1054 nm for the 68 layer PW FOA steering mirror coating for 35° AOI, Ppol. Left and right shaded areas and dashed vertical lines identify optical media, as in Fig. 8.

We returned to the design process, looking for design options based not only on meeting the HR requirements but also on meeting the requirement that the optical electric field intensity behavior within the coating show moderate intensity peaks that rapidly quench within the first ~ 15 coating layers for 527 nm as well as for 1054 nm. The result was a suitable 50 layer design for a coating about 8 μm thick that meets both of these requirements. Figure 10 shows its 25°, 30°, 35°, 40°, and 45° AOI, Ppol reflection spectra near 527 nm and 1054 nm, confirming the PW FOA HR performance specifications (R > 99.6% for 527 nm +/- 3 nm and 1054 nm +/- 6 nm), but now over narrower ranges of wavelengths (R > 99.6% for 523 nm – 533 nm and 1048 nm – 1065 nm) as compared to the 68 layer coating (see Fig. 6; R > 99.6% for 518 nm – 541 nm and 1038 nm – 1084 nm). Meeting such an HR specification within narrower spectral range margins places increased demands on coating process control and achievement of layer pair accuracies in the deposition of the 50 layer coating. On the other hand, the risks of coating system and process failures for the 50 layer deposition are not as high as for the 68 layer deposition.

Figure 11 shows the 527 nm and 1054 nm electric field behaviors within the 50 layer coating for 35° AOI and both Ppol and Spol, and they all meet the design goal of exhibiting rapid quenching into the coating. We include the Spol intensities in Fig. 11 to contrast them with

the Ppol intensities. The intensity patterns for both 527 nm and 1054 nm are similar in their moderate peaks that quickly quench within the coating. But, in each case, the Spol intensities are slightly lower than the Ppol intensities within the coating but peak much higher in the incident medium just in front of the coating. The Spol intensities also reach near zero intensity minima at the coating layer interfaces and at the interface between the coating and the incident medium, and show no intensity jumps. The Ppol intensities, on the other hand, exhibit intensity jumps at the media interfaces, particularly at the interface between the coating and the incident medium. These Spol and Ppol intensity behaviors are characteristic of HR coating designs like the 50 layer design, and their differences are due to

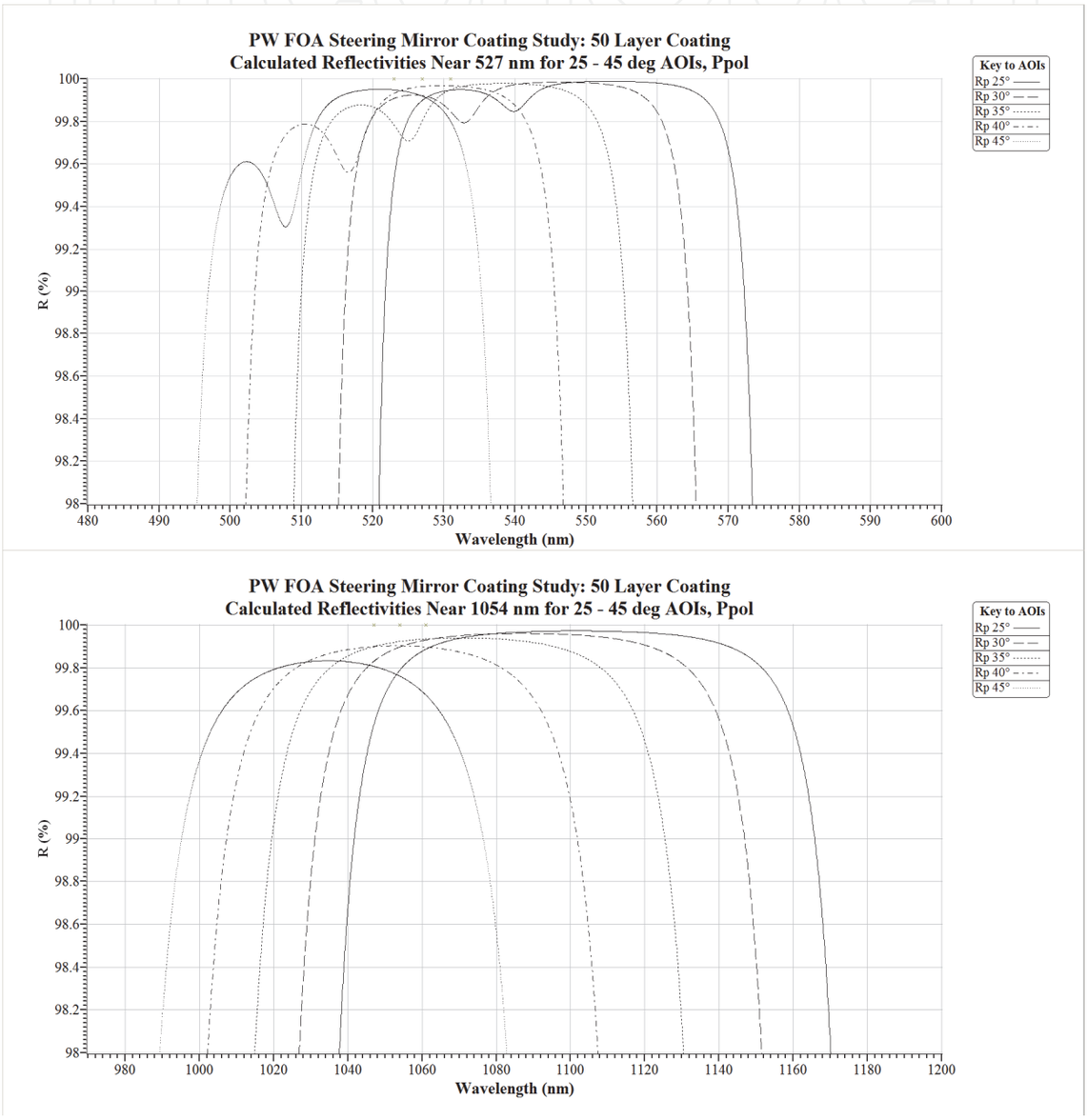

Fig. 10. Calculated reflectivities for Ppol at 25°, 30°, 35°, 40° and 45° AOIs and wavelengths near 527 nm (top figure) and 1054 nm (bottom figure) according to the 50 layer coating design for the PW FOA steering mirror.

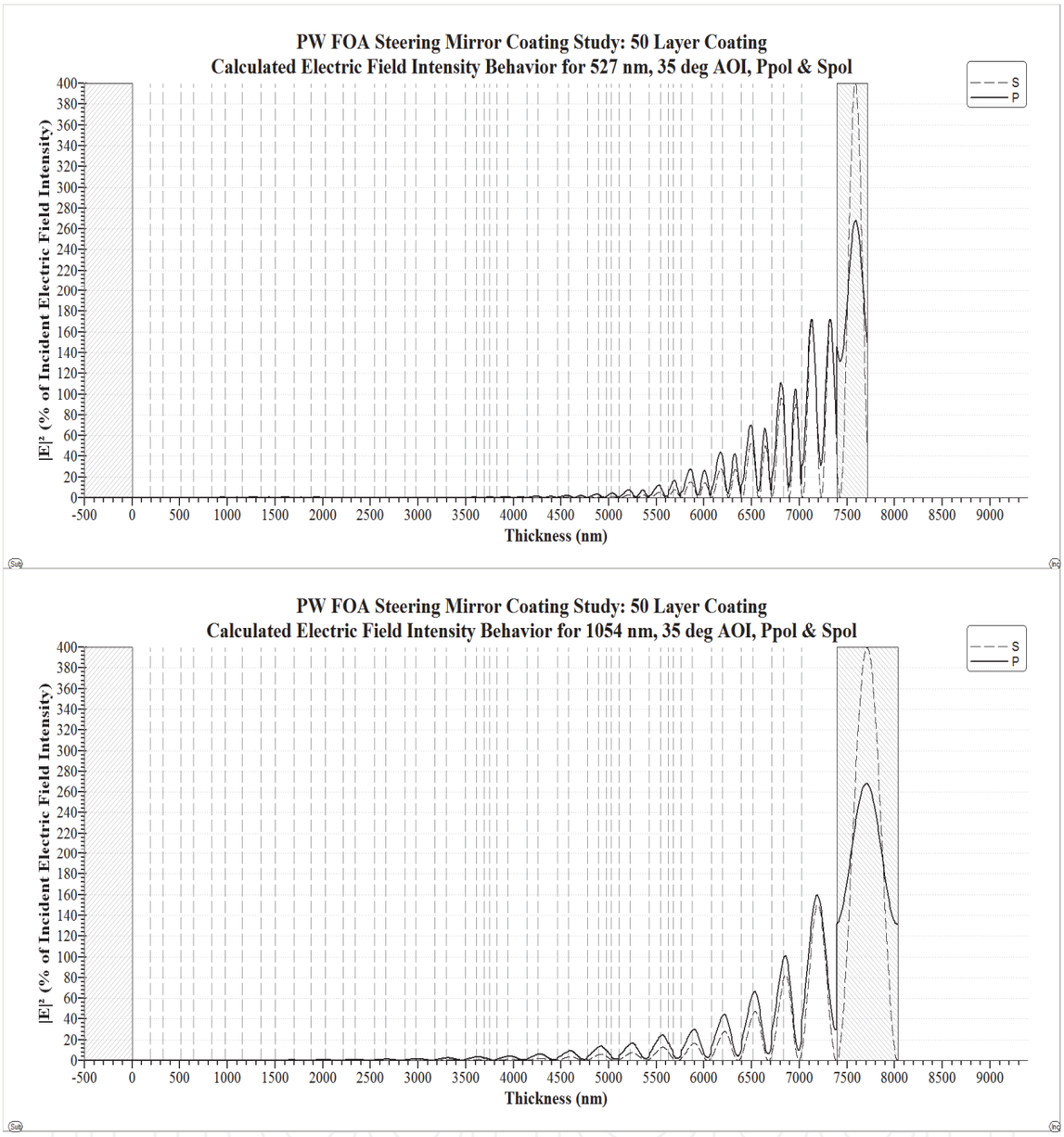

Fig. 11. Calculated electric field intensity at 527 nm (top figure) and 1054 nm (bottom figure) for the 50 layer PW FOA steering mirror coating design for 35° AOI, Ppol and Spol. Left and right shaded areas and dashed vertical lines identify optical media, as in Fig. 8.

the differences in boundary conditions satisfied by Spol and Ppol components of the optical electric field at media interfaces (Born & Wolf, 1980; Bellum, et al., 2011). In any case, because Ppol intensities exhibit jumps at media interfaces and are somewhat higher than the Spol intensities for these HR coatings, their Ppol LIDTs should be lower than their Spol counterparts. That is why our LIDT tests of HR coatings are usually with Ppol, providing a more conservative assessment of the coatings' resistance to laser damage. Another difference between Ppol and Spol behaviors for HR coatings is that the Spol reflectivities are usually higher, and remain high over a broader spectral range, than is the case for their Ppol

reflectivity counterparts. Thus, the 50 layer coating will meet the stringent HR performance specifications of the PW FOA steering mirror for Spol within spectral margins near 527 nm and 1054 nm that are wider than the very narrow spectral margins (see Fig. 10) in which it meets those specifications for Ppol.

The LIDTs are indeed high at both 1064 nm and 532 nm for this 50 layer PW FOA steering mirror HR coating as confirmed by the LIDT test results of Fig. 12 for 35° AOI, Ppol, showing in this case that the 1064 nm LIDT is 76 J/cm² (based on propagating damage as opposed to non-propagating damage sites exceeding 25) and the 532 nm LIDT is ~ 12 J/cm² (based on both propagating and non-propagating damage criteria since, at 13 J/cm², non-propagating damage sites had accumulated to 43 and propagating damage had also occurred). The 50 layer coating's 1064 nm LIDT of 76 J/cm² at 35° AOI, Ppol is similar to its counterpart (>79 J/cm²) for the 68 layer coating, but its 532 nm LIDT of ~ 12 J/cm² at 35° AOI, Ppol is nearly 5 times higher than the 2.5 J/cm² LIDT of its 68 layer coating counterpart. The corresponding LIDT results at 25°, 30°, 40° and 45° AOIs are, respectively, 16 J/cm², 16 J/cm², 19 J/cm² and 19 J/cm² at 532 nm; and, respectively, 70 J/cm², 67 J/cm², 82 J/cm² and 64 J/cm² at 1064 nm. These are consistent with their 35° AOI counterparts. This is a satisfying result for the 50 layer coating, indicating that both its 1054 nm and 527 nm LIDTs meet the laser damage resistance required by ns class Z-Backlighter laser pulses over the entire 24° – 47° range of AOIs.

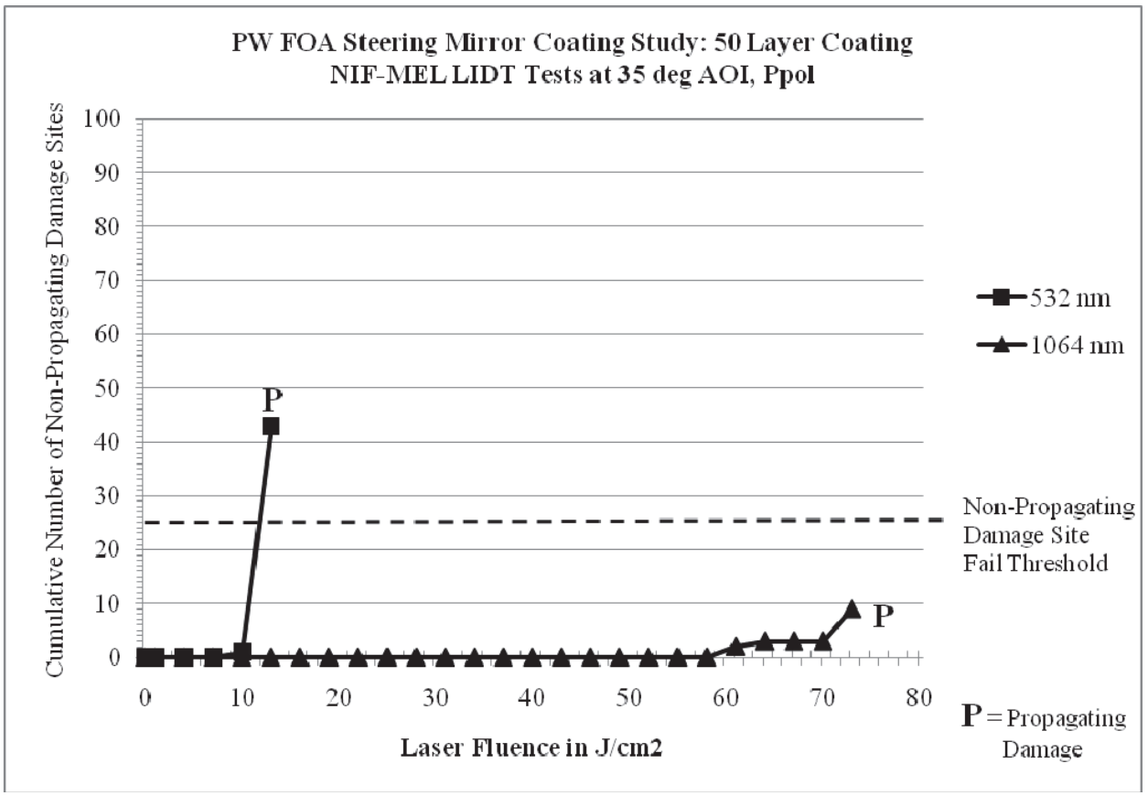

Fig. 12. NIF-MEL LIDT test results at 532 nm and 1064 nm, and 35° AOI, Ppol, for the 50 layer PW FOA steering mirror coating.

This case study for the complex and demanding PW FOA steering mirror HR coating requirements demonstrates the critical role that coating design plays in obtaining coatings

that not only meet reflection or transmission specifications, but do so in terms of electric field behaviors within the coating that favor the highest achievable LIDTs. In our study of electric field intensity behaviors for AR coatings (Bellum et al., 2011), we found that the interference of forward and backward propagating components of light leads to electric field intensity behaviors quite different from those for HR coatings, consistent with AR coating design goals of transmitting rather than reflecting incident light. We also found interesting correlations for AR coatings between their LIDTs and the behaviors of the optical electric fields within them, and especially the behaviors of Ppol intensity jumps at coating layer boundaries in the case of non-normal AOIs (Bellum et al., 2011).

8. AR coating case study: Reflectivities and uniformity of AR coatings for a TW diagnostic beamsplitter

The next case study highlights aspects of reflectivity and uniformity of coatings for meter-class, high intensity laser optics in the context of the Side 1 and Side 2 AR coatings of a diagnostic beamsplitter for the TW class Z-Beamlet laser beam at 527 nm and 22.5° AOI. This beamsplitter and diagnostic of the 527 nm beam are located just beyond where it is generated by means of frequency doubling of the 1054 nm beam in a large KDP crystal. Because the frequency doubling process is about 70% efficient, the actual beam emerging from the KDP crystal consists of the 527 nm TW beam as its primary component, comprising ~ 70% of the total beam intensity and the one of interest on target, and a residual 1054 nm beam of much lower intensity whose role on target is relatively minor and inconsequential. The schematic of Fig. 13 depicts the 527 nm and 1054 nm components of the TW laser beam together with the beamsplitter, which is a 61.5 cm diameter, fused silica optic with ~ 50 cm diameter central clear aperture.

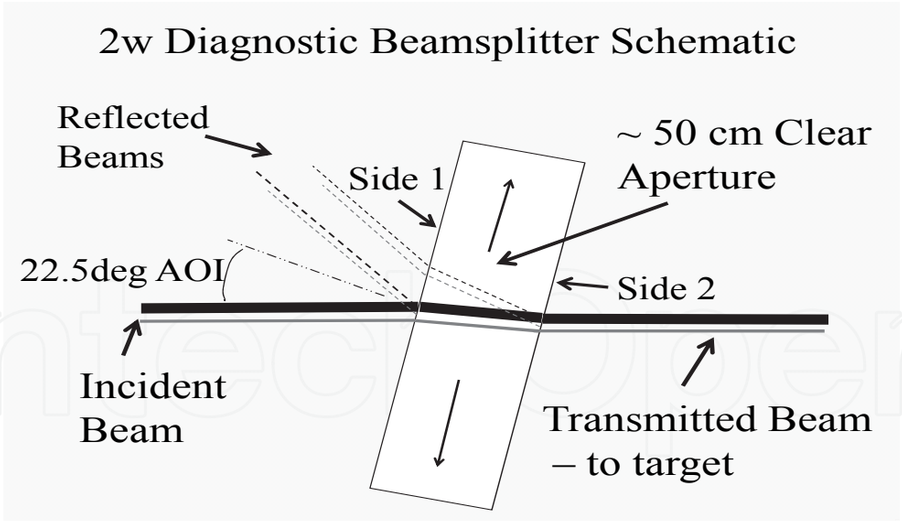

Fig. 13. Schematic diagram of the diagnostic beamsplitter. The solid and dashed lines in black represent the laser beam components at 527 nm while the solid and dashed lines in gray represent the laser beam components at 1054 nm.

The purpose of the Side 1 AR coating of the beamsplitter is to sample the 527 nm TW beam, which undergoes diagnostics of transverse intensity and phase that faithfully match those of the 527 nm TW beam to the extent that the reflectivity at 527 nm across the Side 1 clear aperture is uniform. To do this, the Side 1 coating must not only offer very uniform

performance over the beamsplitter clear aperture but also must strike a balance between excellent and merely good AR performance at 527 nm. An excellent 527 nm AR, with reflectivity in the range of ~ 0.14%, would be desirable for minimizing intensity losses and delivering the 527 nm TW beam to target with maximum intensity in the target focal volume. But such low reflectivities afford insufficient intensity in the sample beam to ensure reliable diagnostics. So, in the design of this Side 1 AR coating, we had to sacrifice somewhat the excellence of the 527 nm AR performance, to a level allowing adequate sample intensity for good diagnostics at the expense of a higher loss of transmitted TW intensity than we would like. Accordingly, we set a design goal for the Side 1 AR coating to reflect 527 nm light in the range of 0.5% - 1.0%. For 1054 nm, the Side 1 coating needs to provide an excellent AR to minimize the amount of reflected light at 1054 nm co-propagating with the 527 nm sample beam and possibly interfering with the 527 nm diagnostics.

The Side 2 AR coating, unlike that of Side 1, does not provide a sample of the 527 nm TW beam for diagnostics. Rather, it should offer excellent 527 nm AR so as to add the least amount intensity loss as possible to the losses incurred by the 527 nm TW beam at Side 1. On the other hand, the amount of the 1054 nm residual component of the TW beam reaching the target is not critical and the 1054 nm AR property of the Side 2 coating is also not critical, but need only be in the range of excellent to good in order to keep 1054 nm light reflected by Side 2 at reasonably low intensities. In summary, we designed the coatings for this beamsplitter to meet AR performances at the 22.5° AOI as follows: for Side 1, 0.5% - 1.0% reflectivity at 527 nm and ~ 0.15% or less reflectivity at 1054 nm; and, for Side 2, ~ 0.15% or less reflectivity at 527 nm and 0.5% - 1.5% reflectivity at 1054 nm. We reported the actual layer thicknesses of these Side 1 and Side 2 AR coatings in our previous paper on correlations between LIDTs and electric field intensity behaviors for AR coatings (Bellum et al., 2011). A slight wedge angle between Sides 1 and 2 prevents 527 nm and 1054 nm components of light reflected by Side 2 from entering the 527 nm diagnostic beam train and possibly interfering with the diagnostics.

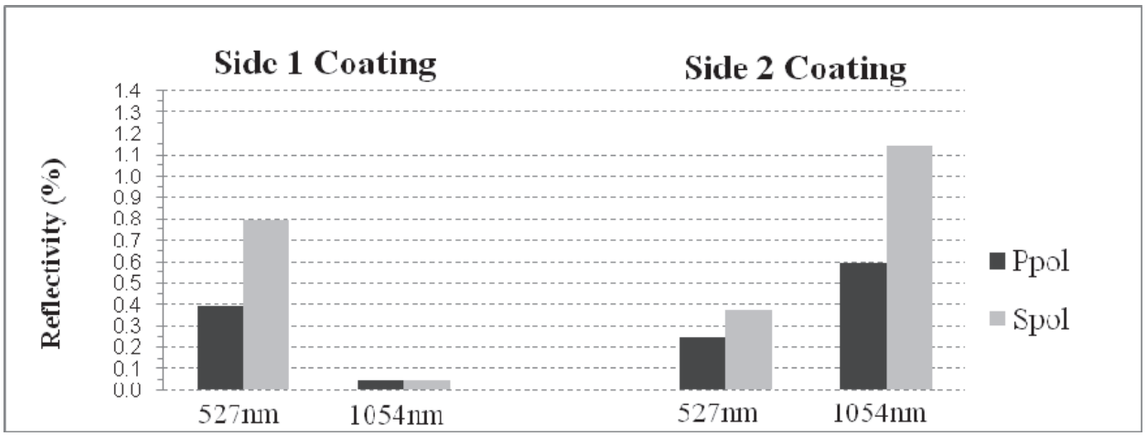

Fig. 14. Measured reflectivities at 527 nm and 1054 nm of the as-deposited Side 1 and Side 2 AR coatings of the diagnostic beamsplitter at its 22.5° use AOI for both Ppol and Spol.

Figure 14 shows the measured reflectivities at 527 nm and 1054 nm for the actual, as-deposited, Side 1 and Side 2 AR coatings at their 22.5° use AOI for both Ppol and Spol. These measurements were on small coated witness substrates using the Sandia reflectometer in a configuration that can also accommodate large, meter-class, optical substrates. We met

our coating design goals for Side 1, with reflectivities of ~ 0.4% for Ppol and ~ 0.8% for Spol in the case of 527 nm, and ~ 0.045% for both Ppol and Spol in the case of 1054 nm; and for Side 2 at 1054 nm, with a reflectivity of ~ 0.6% for Ppol and ~ 1.14% for Spol. But our Side 2 reflectivity at 527 nm, of ~ 0.24% for Ppol and ~ 0.37% for Spol, while reasonably low, is about 2 times larger than our design goal of 0.15% or less, indicating that we need to improve on our Side 2 AR coating design in this respect.

Fig. 15 presents measured results for the uniformity of these two coatings. These measurements are based on broadband reflection spectra of the coatings, from roughly 400 nm to 900 nm, recorded in 2 cm intervals along a 5 cm wide uniformity witness optic spanning the full 94 cm diameter of one of the three equivalent planetary fixtures during the Side 1 and Side 2 product coating runs. Another of these planetary fixtures held the diagnostic beamsplitter product optic during these runs. We track the wavelengths of spectral peaks or valleys, which are easily identifiable features of the spectra, measuring them at each 2 cm interval along the planetary diameter according to the percent deviations from their average values. As Fig. 15 shows, the averages of these spectral peak and valley percent deviations are within +/- 0.5% over the central 60 cm of the planet diameter for both

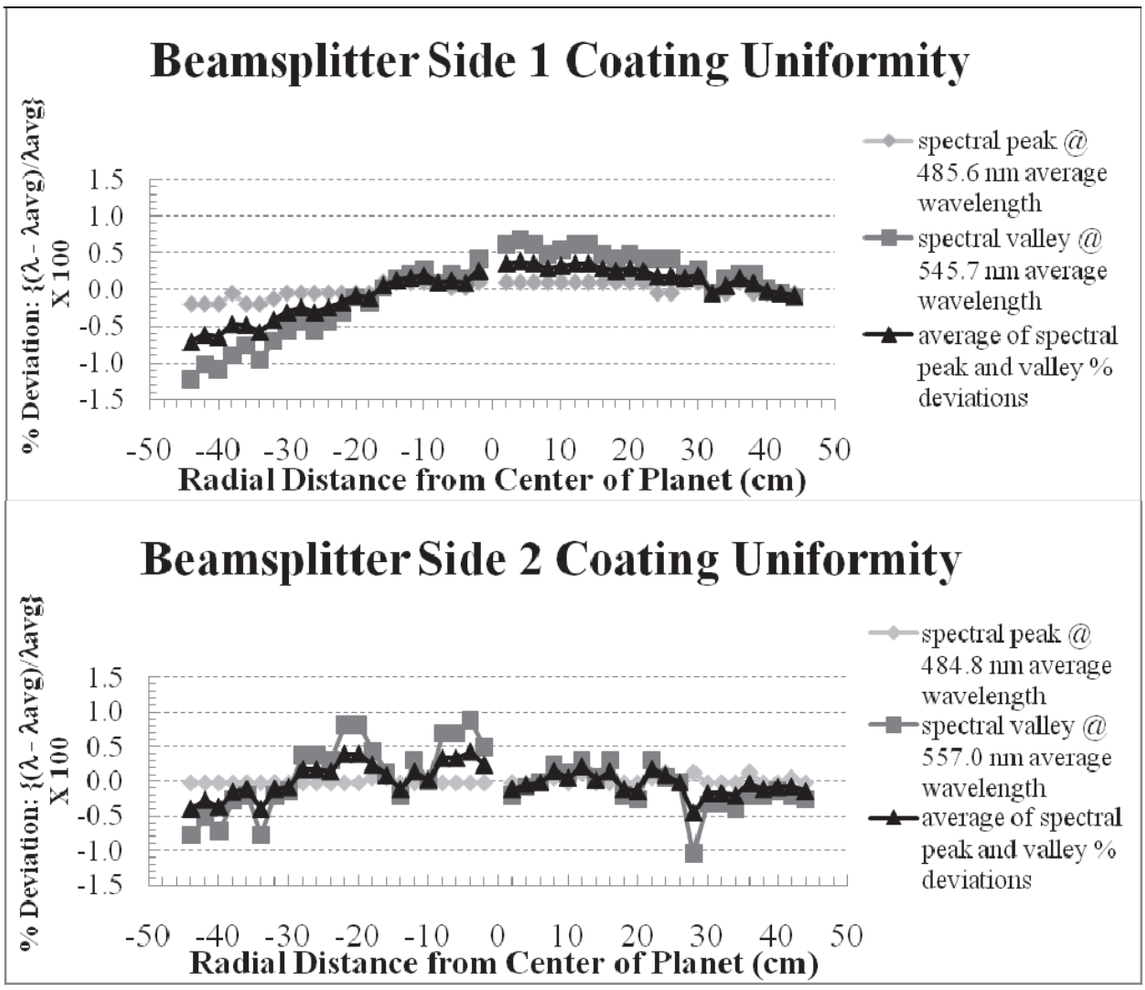

Fig. 15. Measured uniformity for the diagnostic beamsplitter Side 1 (top figure) and Side 2 (bottom figure) AR coatings. See text for details.

the Side 1 and Side 2 coatings. This high level of uniformity, which is typical for our coatings, is critical to insuring that the transverse phase and relative intensity properties of the 527 nm sample beam reflected from Side 1 closely match those of the 527 nm TW laser beam incident on the diagnostic beamsplitter. Only with such accurate matching of phase and relative intensity between the 527 nm sample and TW beams will the diagnostics of the sample beam reliably describe those of its TW counterpart. The Spol and Ppol LIDTs of these Side 1 and Side 2 diagnostic beamsplitter AR coatings measured in the NIF-MEL protocol at their 22.5° use AOI are > 10 J/cm² at 532 nm and > 38 J/cm² at 1064 nm, as we reported previously (Bellum et al., 2011), and are thus adequate to protect against laser damage in the Z-Backlighter laser beam trains.

9. Conclusion

This chapter is an in-depth overview of the production of high LIDT optical coatings for PW class laser pulses. Lasers that generate such ultra-high intensity pulses use various approaches involving large energies per pulse and/or extremely short pulse durations, including the use of CPA techniques which have revolutionized ultra-high intensity laser technology. The successful operation of these lasers depends on optical coatings of the highest possible LIDTs to insure that the ultra-high intensity laser pulses, regardless of their pulse duration/energy combination, are able to propagate along the laser beam train without causing damage or aberrations. Our focus is on producing these high LIDT optical coatings on the large, meter-class optics required by the important category of ultra-high intensity lasers that use large cross section beam trains to accommodate large energies per pulse. Such large scale lasers were the earliest sources of PW class pulses and continue as important sources of PW pulses not only in the ns regime but also in the sub-ps regime by means of CPA. Sandia's Z-Backlighter TW and PW lasers, with their large cross section beam trains supporting ns pulses at 527 nm and 1054 nm and sub-ps, CPA pulses at 1054 nm, and its Large Optics Coating Operation together provide an excellent context for our overview of high LIDT coatings.

The LIDT of an optical coating depends not only on the resistance of the coating materials to laser damage but also on the design of the coating, on the techniques of keeping the optic surface free of particulates or contamination and of preparing it for coating, and on the coating process itself. Even a single particulate on an optic surface prior to coating can initiate laser damage and undermine an otherwise high LIDT of the coated surface. For this reason, a coating operation for producing high LIDT coatings must use a Class 100 or cleaner environment with excellent downward laminar flow of the clean air. In this regard, integrating the coating chamber into the Class 100 environment, with appropriate clean room curtain partitions, is also crucial. Of related importance is to transfer an optic into the coating chamber in a way that prevents the surface to be coated from exposure to particulates or contamination from the coating chamber or tooling. Proper coating process control is also important to obtaining coatings with high LIDTs. This includes deposition of hafnia by means of e-beam evaporation of hafnium metal in an oxygen back pressure, and use of IAD and temperature control of the coating chamber/substrate to tailor the molecular dynamics of coating formation as a means of fine tuning the coating's stress and density. Planetary motion of the substrates undergoing coating is necessary for obtaining good uniformity of coatings over large substrate surfaces. Coating large dimension optics poses unique challenges related to coating material depletion and the risk of system and process failures associated with producing uniform coatings in large coating chambers, and we summarize these large optics coating production challenges.

Regarding polishing, washing and cleaning of an optic prior to coating it, we point out that residual amounts of the polishing compound embedded in the microstructure of the polished surface can compromise the LIDT of the coated surface. As a result, the wash process must remove not only surface contamination but also polishing compound embedded in the microstructure of the polished optical surface. Using a wash protocol that includes an alumina slurry wash step in addition to mild detergent wash and clear water rinse steps does partially remove residual polishing compound from optic surfaces, and leads to improved LIDTs of AR coatings on those surfaces.

Useful LIDT tests are essential to the development and fielding of high LIDT optical coatings. Important here is to take into account the differences between the LIDT test laser conditions and the use laser conditions. This means that results of LIDT tests require careful interpretation in determining how they relate and apply to the design and performance of a given PW class laser. Our evaluation of the NIF-MEL LIDT tests and our in-house LIDT tests, and of how they relate to the Z-Backlighter TW and PW laser conditions, illustrates this. A comprehensive summary of the results of these LIDT tests on Sandia AR and HR coatings, for ns class pulses at 532 nm and 1064 nm and sub-ps class pulses at 1054 nm, shows that the LIDTs are high and adequate to insure that the coatings can stand up to the laser fluence levels of the PW class pulses in the Z-Backlighter beam trains.

Electric field behavior due to interference of forward and backward propagating components of light in a coating can be very different for different coating designs that meet the same reflectivity specifications, and not all field behaviors favor high LIDTs. Our first case study clearly illustrates this with the PW FOA steering mirror coating according to a 68 layer design and a 50 layer design. Both designs meet the mirror's extremely challenging reflection specifications ($R > 99.6$ % for 527 nm and 1054 nm for Spol and Ppol at AOIs from 24^o to 47^o) but the LIDTs at 527 nm are ~ 5 times larger for the 50 layer coating than for the 68 layer coating. This correlates with the moderate electric field intensity peaks at 527 nm that quench rapidly into the coating for the 50 layer design in contrast to the stronger 527 nm electric field intensity peaks, at ~ 200 % of the incident intensity and deep within the coating, for the 68 layer design. Some electric field behaviors afford higher LIDTs than others, and it is possible to design a coating that not only meets reflectivity requirements but that also is characterized by electric field intensities that enhance the LIDT of the coating.

Our second case study, of the Side 1 and Side 2 AR coatings of the diagnostic beamsplitter for the Z-Backlighter pulses at 527 nm, highlights reflectivity performance and uniformity which, though always important for large optics coatings, are particularly critical for diagnostic beamsplitter coatings since the validity of the beam diagnostics depends on them. Because partial reflection of the 527 nm laser beam by the beamsplitter produces the low intensity sample beam that undergoes the beam diagnostic tests, this partial reflection process must accurately preserve the transverse phase and relative intensity of the 527 nm laser beam over its entire cross section in order for it to be reliably described by the diagnostics of the sample beam. The Side 1 and Side 2 beamsplitter AR coatings of this case study do exhibit excellent uniformity and their designs match subtle reflectivity requirements, insuring beam diagnostics based on appropriate partial reflection with integrity of transverse phase and relative intensity. The coatings also account for secondary pulses at 1054 nm co-propagating with the primary pulses at 527 nm, a dual beam situation not uncommon for PW class lasers as a by-product of frequency doubling to produce the primary laser beam.

This chapter has covered key aspects of producing high LIDT optical coatings for PW class laser pulses. We hope it is of practical value in helping researchers in the field of ultra-high intensity lasers to navigate the design and production issues and considerations for high LIDT coatings.

10. Acknowledgement

Sandia National Laboratories is a multi-program laboratory managed and operated by Sandia Corporation, a wholly owned subsidiary of Lockheed Martin Corporation, for the U.S. Department of Energy's National Nuclear Security Administration under contract DE-AC04-94AL85000.

11. References

American National Standards Institute (2006). ANSI/OEOSC OP1.002-2006, Optics and Electro-Optical Instruments - Optical Elements and Assemblies - Appearance Imperfections. Available from ANSI eStandards Store: http://www.webstore.ansi.org/default.aspx.

American National Standards Institute (2008). ISO 10110-7:2008(E), Optics and photonics – Preparation of drawings for optical elements and systems – Part 7: Surface imperfection tolerances. Available from ANSI eStandards Store: http://www.webstore.ansi.org/default.aspx.

Bellum, J., Kletecka, D., Rambo, P., Smith, I., Kimmel, M., Schwarz, J., Geissel, M., Copeland, G., Atherton, B., Smith, D., Smith, C. & Khripin, C. (2009). Meeting thin film design and production challenges for laser damage resistant optical coatings at the Sandia Large Optics Coating Operation. *Proc. of SPIE*, Vol.7504, 75040C, ISBN 9780819478825, Boulder, Colorado, USA, September 2009.

Bellum, J., Kletecka, D., Kimmel, M., Rambo, P., Smith, I., Schwarz, J., Atherton, B., Hobbs, Z. & Smith, D. (2010). Laser damage by ns and sub-ps pulses on hafnia/silica anti-reflection coatings on fused silica double-sided polished using zirconia or ceria and washed with or without an alumina wash step. *Proc. of SPIE*, Vol.7842, 784208, ISBN 9780819483652, Boulder, Colorado, USA, September 2010.

Bellum, J., Kletecka, D., Rambo, P., Smith, I., Schwarz, J. & Atherton, B. (2011). Comparisons between laser damage and optical electric field behaviors for hafnia/silica antireflection coatings. *Appl. Opt.*, Vol.50, 9, March 2011, pp. C340-C348, ISSN 0003-6935.

Born, M. & Wolf, E. (1980). *Principals of Optics* (6th Edition), Pergamon Press Inc., ISBN 0-08-026481-6, New York.

Do, B. T. & Smith, A. V. (2009). Deterministic single shot and multiple shots bulk damage thresholds for doped and undoped, crystalline and ceramic YAG. *Proc. of SPIE.* Vol.7504, 75041O, ISBN 9780819478825, Boulder, Colorado, USA, September 2009.

Fournet, C., Pinot, B., Geenen, B., Ollivier, F., Alexandre, W., Floch, H. G., Roussel, A., Cordillot, C. & Billon, D. (1992). High damage threshold mirrors and polarizers in the ZrO_2/SiO_2 and HfO_2/SiO_2 dielectric systems. *Proc. of SPIE*, Vol.1624, pp. 282-293, ISBN 9780819407665, Boulder, Colorado, USA, September 1991.

Kimmel, M., Rambo, P., Broyles, R., Geissel, M., Schwarz, J., Bellum, J. & Atherton, B. (2009). Optical damage testing at the Z-Backlighter Facility at Sandia National Laboratories. *Proc. of SPIE*, Vol.7504, 75041G, ISBN 9780819478825, Boulder, Colorado, USA, September 2009.

Kimmel, M., Rambo, P., Schwarz, J., Bellum, J. & Atherton, B. (2010). Dual wavelength laser damage testing for high energy lasers. *Proc. of SPIE*, Vol.7842, 78421O, ISBN 9780819483652, Boulder, Colorado, USA, September 2010.

Maine, P., Strickland, D., Bado, P., Pessot, M. & Mourou, G. (1988). Generation of Ultrahigh Peak Power Pulses by Chirped Pulse Amplification. *IEEE J. Quantum Electron.*, Vol.24, 2, February 1988, pp. 398-403, ISSN 0018 9197.

Menapace, J. A. (2010). Private communication with J. A. Menapace, Lawrence Livermore National Laboratory.

Mourou, G. A. & Umstadter, D. (2002). Extreme Light. *Scientific American*, Vol.286, 5, May 2002, pp. 81-86, ISSN 0036-8733.

Mourou, G. & Tajima, T. (2011). More Intense, Shorter Pulses. *Science*, Vol.331, 6013, January 2011, pp. 41-42, ISSN 0036-8075 (print), ISSN 1095-9203 (online).

National Ignition Facility (2005). Small Optics Laser Damage Test Procedure. NIF Tech. Rep. MEL01-013-0D, Lawrence Livermore National Laboratory, Livermore, California.

Perry, M. D. & Mourou, G. (1994). Terawatt to Petawatt Subpicosecond Lasers. *Science*, Vol.264, 5161, May 1994, pp. 917-924, ISSN 0036-8075 (print), ISSN 1095-9203 (online).

Rambo, P. K., Smith, I. C., Porter Jr., J. L., Hurst, M. J., Speas, C. S., Adams, R. G., Garcia, A. J., Dawson, E., Thurston, B. D., Wakefield, C., Kellogg, J. W., Slattery, M. J., Ives III, H. C., Broyles, R. S., Caird, J. A., Erlandson, A. C., Murray, J. E., Behrendt, W. C., Neilsen, N. D. & Narduzzi, J. M. (2005). Z-Beamlet: a multikilojoule, terawatt-class laser system. *Appl. Opt.*, Vol.44, 12, April 2005, pp. 2421-2430, ISSN 0003-6935.

Schwarz, J., Rambo, P., Geissel, M., Edens, A., Smith, I., Brambrink, E., Kimmel, M. & Atherton, B. (2008). Activation of the Z-Petawatt laser at Sandia National Laboratories. *Journal of Physics: Conference Series*, Vol.112, 032020, ISSN 1742-6596, Kobe, Japan, September 2007.

Sinars, D. B., Cuneo, M. E., Bennett, G. R., Wenger, D. F., Ruggles, L. E., Vargas, M. F., Porter, J. L., Adams, R. G., Johnson, D. W., Keller, K. L., Rambo, P. K., Rovang, D. C., Seamen, H., Simpson, W. W., Smith, I. C. & Speas, S. C. (2003). Monochromatic x-ray backlighting of wire-array z-pinch plasmas using spherically bent quartz crystals. *Rev. Sci. Instr.*, Vol.74, 3, March 2003, pp. 2202-2205, ISSN 0034-6748.

Smith, D. J., McCullough, M., Smith, C., Mikami, T. & Jitsuno, T. (2008). Low stress ion-assisted coatings on fused silica substrates for large aperture laser pulse compression gratings. *Proc. of SPIE*, Vol.7132, 71320E, ISBN 9780819473660, Boulder, Colorado, USA, September 2008.

Stolz, C. J. & Genin, F. Y. (2003). Laser Resistant Coatings, In: *Optical Interference Coatings*, Kaiser, N. & Pulker, H. K. (Eds.), pp. 309-333, Springer-Verlag, ISBN 3-540-00364-9, Berlin/Heidelberg.

Stolz, C. J., Thomas, M. D. & Griffin, A. J. (2008). BDS thin film damage competition. *Proc. of SPIE*, Vol. 7132, 71320C, ISBN 9780819473660, Boulder, Colorado, USA, September 2008.

Strauss, G. N. (2003). Mechanical Stress in Optical Coatings, In: *Optical Interference Coatings*, Kaiser, N. & Pulker, H. K. (Eds.), pp. 207-229, Springer-Verlag, ISBN 3-540-00364-9, Berlin/Heidelberg.

Strickland, D. & Mourou, G. (1985). Compression of amplified chirped optical pulses. *Opt. Commun.*, Vol.56, 3, December 1985, pp.219-221, ISSN 0030-4018.

Tajima, T., Mourou, G. A. & Habs, D. (2010). Highest intensities, shortest pulses: Towards new physics with the Extreme Light Infrastructure. *Optik & Photonik*, Vol.5, 4, December 2010, pp. 24-29, ISSN 2191-1975 (online).

Wood, R. M. (Ed.). (1990). *Selected Papers on Laser Damage in Optical Materials*, SPIE Press Milestone Series Vol.MS24, ISBN 9780819405432, Bellingham, Washington.

Wood, R. M. (2003). *Laser-Induced Damage of Optical Materials*, Institute of Physics Publishing, ISBN 0 7503 0845 1, Bristol & Philadelphia.

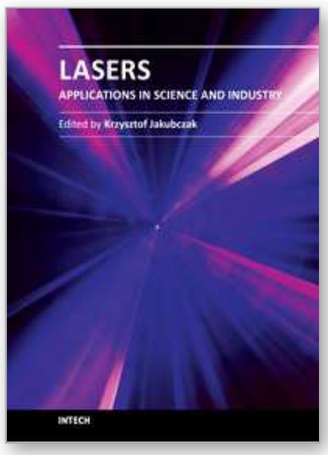

Lasers - Applications in Science and Industry
Edited by Dr Krzysztof Jakubczak

ISBN 978-953-307-755-0
Hard cover, 276 pages
Publisher InTech
Published online 09, December, 2011
Published in print edition December, 2011

The book starts with basic overview of physical phenomena on laser-matter interaction. Then it is followed by presentation of a number of laser applications in the nano-particles and thin films production, materials examination for industry, biological applications (in-vitro fertilization,tissue ablation) and long-range detection issues by LIDARs.

How to reference
In order to correctly reference this scholarly work, feel free to copy and paste the following:

John Bellum, Patrick Rambo, Jens Schwarz, Ian Smith, Mark Kimmel, Damon Kletecka and Briggs Atherton (2011). Production of Optical Coatings Resistant to Damage by Petawatt Class Laser Pulses, Lasers - Applications in Science and Industry, Dr Krzysztof Jakubczak (Ed.), ISBN: 978-953-307-755-0, InTech, Available from: http://www.intechopen.com/books/lasers-applications-in-science-and-industry/production-of-optical-coatings-resistant-to-damage-by-petawatt-class-laser-pulses

INTECH
open science | open minds

InTech Europe
University Campus STeP Ri
Slavka Krautzeka 83/A
51000 Rijeka, Croatia
Phone: +385 (51) 770 447
Fax: +385 (51) 686 166
www.intechopen.com

InTech China
Unit 405, Office Block, Hotel Equatorial Shanghai
No.65, Yan An Road (West), Shanghai, 200040, China
中国上海市延安西路65号上海国际贵都大饭店办公楼405单元
Phone: +86-21-62489820
Fax: +86-21-62489821

IntechOpen